

# Integrated and global pseudotargeted metabolomics strategy applied to screening for quality control markers of *Citrus* TCMs

Yisong Shu<sup>1,2</sup> · Zhenli Liu<sup>3</sup> · Siyu Zhao<sup>1,2</sup> · Zhiqian Song<sup>3</sup> · Dan He<sup>1,2</sup> · Menglei Wang<sup>1,2</sup> · Honglian Zeng<sup>1,2</sup> · Cheng Lu<sup>4</sup> · Aiping Lu<sup>4,5</sup> · Yuanyan Liu<sup>1</sup>

Received: 28 February 2017 / Revised: 13 May 2017 / Accepted: 23 May 2017 / Published online: 10 July 2017  
© Springer-Verlag Berlin Heidelberg 2017

**Abstract** Traditional Chinese medicine (TCM) exerts its therapeutic effect in a holistic fashion with the synergistic function of multiple characteristic constituents. The holism philosophy of TCM is coincident with global and systematic theories of metabolomics. The proposed pseudotargeted metabolomics methodologies were employed for the establishment of reliable quality control markers for use in the screening strategy of TCMs. Pseudotargeted metabolomics integrates the advantages of both targeted and untargeted methods. In the present study, targeted metabolomics equipped with the gold standard RRLC-QqQ-MS method was employed for in vivo quantitative plasma pharmacochimistry study of characteristic prototypic constituents. Meanwhile, untargeted metabolomics using UHPLC-QE Orbitrap HRMS with better specificity and selectivity was employed for identification of untargeted metabolites in the complex plasma matrix. In all, 32 prototypic metabolites were quantitatively determined, and 66 biotransformed metabolites were convincingly identified after being orally administered with standard extracts of four

labeled *Citrus* TCMs. The global absorption and metabolism process of complex TCMs was depicted in a systematic manner.

**Keywords** Pseudotargeted metabolomics · Citrus TCMs · Metabolites identification · Drug metabolism · QC-markers

## Introduction

Traditional Chinese medicine (TCM) is widely used in China and other Asian countries, for the prevention, diagnosis, treatment of disease or to regulate human function, and has gradually become an effective supplement therapy in the West. TCM is a unique medical system with the significant characteristic of pursuing an overall therapeutic effect with a multi-target treatment. It consists of multiple major or minor constituents that can regulate the balance and homeostasis of the body in a holistic fashion. Quantitative analysis with charac-

**Electronic supplementary material** The online version of this article (doi:10.1007/s00216-017-0428-1) contains supplementary material, which is available to authorized users.

✉ Zhenli Liu  
zhenli\_liu@sina.com

✉ Cheng Lu  
lv\_cheng0816@163.com

✉ Aiping Lu  
lap64067611@126.com

✉ Yuanyan Liu  
yyliu\_1980@163.com

<sup>2</sup> State Key Laboratory of Bioactive Substance and Function of Natural Medicines, Institute of Materia Medica, Chinese Academy of Medical Sciences and Peking Union Medical College, Beijing, China

<sup>3</sup> Institution of Basic Theory, China Academy of Chinese Medical Sciences, Beijing 100700, China

<sup>4</sup> Institute of Basic Research in Clinical Medicine, China Academy of Chinese Medical Sciences, Beijing 100700, China

<sup>5</sup> School of Chinese Medicine, Hong Kong Baptist University, Kowloon, Hongkong, China

<sup>1</sup> School of Chinese Materia Medica, Beijing University of Chinese Medicine, Beijing 100029, China

teristic constituents is recognized as the prevalent method for quality control of TCM. Generally, single or myriad available constituents contained in the TCM were selected as quality control markers (QC-markers) for quantitative determination, which were responsible for overall pharmacological efficacy. However, these markers may not represent the characteristic or bioactivity of the specific TCM. Therefore, an effective screening strategy for QC-markers that can truly reflect the intrinsic properties of TCM has run into the bottleneck of TCM's modernization, and has become an urgent issue. Since TCM is based on "holism" philosophy, it is philosophically conceivable that metabolomics techniques can provide important information relevant to TCM [1]. Metabolomics has employed global profiling methods for the comprehensive analysis of altered metabolites, providing insights into the global state of the entire metabolic process, which coincides well with the integrity and systemic features of TCMs.

In the present research, a pilot study was performed using four closely related *Citrus* TCMs (e.g., Zhishi, Zhiqiao, Qingpi, and Chenpi) for a performance evaluation as well as a rational screening strategy for QC-markers of other TCMs. *Citrus* plants, which are herbs of homology of medicine and food, are of great interest because they contain large amounts of dietary phenoloids possessing important therapeutic properties for human health, and *Citrus* fruits and their juices are consumed in large quantities around the world [2, 3]. The contents of bioactive phenoloid constituents and profiles in *Citrus* juices vary greatly with the type of fruit. The four *Citrus* TCMs mentioned above are used as drugs for regulating Qi flow and for strengthening the spleen and stomach since ancient times, while their actual clinical applications in China are varied but their QC-markers are rough and similar. Thus, it is important to screen for the representative QC-markers of *Citrus* TCMs both characteristically and bioactively in vitro and in vivo to interpret the material basis for their pharmacological effects. Here, a reliable screening strategy for QC-markers was proposed with the following steps: (a) find chemotaxonomic markers characteristic of the specific TCM using a global plant metabolomics method (completed in our previous research); (b) targeted prototype drug metabolomics applied to the improved quantitative plasma pharmacology analysis; (c) untargeted metabolomics applied to unknown metabolites' semi-quantification and identification (b and c are the pseudotargeted metabolomics methodology); (d) integrating the pseudotargeted metabolomics data and text mining to elucidate the rational metabolic pathway and uncover effective QC-markers.

Pseudotargeted metabolomics is a novel strategy integrating the advantages of both targeted and untargeted methods. For targeted metabolite quantification, multiple reaction monitoring (MRM) performed on a triple quadrupole tandem mass

spectrometry (QqQ-MS) is recognized as the gold standard, attributed to its wide linear dynamic range, high sensitivity, and high repeatability, and has been widely applied in targeted metabolomics [4, 5]. In the realm of plasma pharmacology, only drugs being absorbed into the blood are considered and will probably become bioactive constituents. We put forward an improved quantitative plasma pharmacology methodology using a QqQ instrument to determine and compare targeted prototype constituents, which have been validated as characteristic to specific TCMs. However, targeted metabolomics alone are insufficient to discover the in vivo process and biotransformation of complex TCMs, because natural products are often pro-drugs which must undergo metabolic conversion before being active. It is worth noting that the comprehensive identification of unknown metabolites in complex biological matrices is the vital obstacle. Untargeted metabolomics aims to simultaneously measure as many metabolites as possible in a biological specimen. Often, the chemical identities of the MS-resolved peaks are not known a priori. The ultra-high-performance liquid chromatography Q Exactive hybrid quadrupole-orbitrap high-resolution accurate MS (UHPLC-QE Orbitrap HRMS) instrument has remarkable specificity and selectivity in terms of accurate mass identification and has a profound impact on the identification of characteristic metabolites from complex biological matrices. UHPLC-QE Orbitrap HRMS is of particular importance for in vivo metabolomics studies regarding the identification of untargeted metabolites in complex matrices, due to its capacity in distinguishing chemical-specific metabolites by determining the composition of precursor ions and fragment ions elements, which is capable of analyzing a broad range of secondary metabolites [6]. This method constituted a great development for the application of Q Exactive MS in the comprehensive identification and semi-quantification of untargeted metabolites in vivo. In a word, the combined pseudotargeted metabolomics including targeted and untargeted analysis provided a global insight into the complex process of TCMs in the blood.

Therefore, in order to describe the process of these four *Citrus* TCMs in vivo and to clarify the material basis of the therapeutic effects of different *Citrus* TCMs, the medicative ingredients used as the potential QC-markers in *Citrus* TCMs are screened, and the potential metabolic pathways are elucidated and profiled in rat plasma after oral administration. As a result, 32 absorbed prototype constituents were quantitatively determined in rat plasma after oral administration with standard vehicles of four labeled *Citrus* TCMs. The plasma migrating performance and potential correlations were analyzed between in vitro and in vivo concentrations of prototype constituents. This comparison indicated that the absorption of prototypic constituents exhibited obvious structure dependence. Sixty-six drug metabolites were detected and identified through deconvolution and normalization of complex spectra

collected from the QE Orbitrap HRMS instrument. Based on the integrated pseudotargeted metabolomics data, a large number of metabolites from general metabolic pathways depended largely on the interaction with drug metabolizing enzymes, the constituents' inherent property, I or II reactions, and the biotransformation of gut microbiota. These results contribute to an effective screening strategy for QC-markers and a better understanding of the *in vivo* exposure of complex TCMs to support further drug development and clinical application.

## Materials and methods

### Chemicals and reagents

HPLC-grade methanol and acetonitrile were obtained from Fisher Scientific (Fair Lawn, NJ, USA). The deionized water was redistilled. Formic acid (HPLC grade, Lot. 095224) was obtained from MREDA Technology Inc. (USA). The reference standards of bergapten and narirutin were obtained from Chengdu Must Bio-Technology Co., Ltd. Hesperidin, naringin, kaempferitrin, diosmin, diosmetin-7-O-glucoside, and sinensetin were obtained from Shanghai Source Leaf Biological Technology Co., Ltd. Eriocitrin, neohesperidin, naringenin, hesperetin, luteolin, rutin, isopimpinellin, and tangeretin were obtained from Tianjin Mark Biological Technology Co., Ltd. 5-Demethylnobiletin, nobiletin, and auraptene were obtained from Nanjing JingZhu Biological Technology Co., Ltd. Rhoifolin, apigenin, apigenin-7-O-glucoside, scoparone, and diosmetin were purchased from the National Institute for Control of Biological and Pharmaceutical Products of China. Poncirin, limonin, nomilin, eriodictyol, xanthotoxol, acacetin, isosakuranetin, and imperatorin were purchased from Beijing fufan Biological Technology Co., Ltd. The purity of the standards was relatively high (i.e., higher than 98%). Deionized water was prepared from distilled water using a Milli-Q water purification system (Millipore, Bedford, MA, USA). All other reagents and chemicals used were of analytical grade.

### Preparation of *Citrus* TCM extract

Each *Citrus* TCM was soaked with 1 L ethanol for 30 min after being smashed into powder. Then, the mixture was boiled for 1 h, and this procedure was repeated three times. The combined aqueous extracts were concentrated in a vacuum rotary evaporator to 1 g/mL (crude herbal dose). The aqueous extracts (1 mL) were diluted in 99 mL of 50% methanol and filtered through a 0.22- $\mu$ m microporous membrane before use.

### Animal and drug administration

Male Sprague-Dawley rats ( $250 \pm 20$  g) were purchased from Beijing Vital River Laboratory Animal Technology Co., Ltd. Animals are housed in a separate cage in a room with automatic control of lighting (12 h light/dark cycles, lights on from 8:00 to 20:00), under controlled temperature (22–25 °C) and relative humidity into the food and water. Experiments, which were conducted in a specific pathogen-free (SPF) grade laboratory, were carried out in accordance with the Guide for the Care and Use of Laboratory Animals as adopted and promulgated by the National Health Ministry of China. Protocols for animal experiments had been approved by the Animal Center of the Institute of Basic Theory, China Academy of Chinese Medical Sciences.

Forty male Sprague-Dawley (SD) rats were randomly separated into four groups and administered a dosage of extracts via gastric gavage once per day, the detailed information about oral daily dose of *Citrus* TCMs (Zhishi, Zhiqiao, Qingpi, and Chenpi) is 3.6 g crude drug (20 times of Chinese Pharmacopoeia dose) per rat.

### Plasma sample collection and pretreatment

Approximately 10 mL blood samples were collected from the abdominal aorta in heparinized tubes at 60 min after dosing. The plasma was separated from blood samples by centrifuging at 10,000 rpm for 15 min and was stored at  $-80$  °C for later analysis. Each 1 mL aliquot of plasma sample was mixed with 3 mL of acetonitrile and vortexed for protein precipitation. After centrifugation at 10,000 rpm for 10 min, the supernatant was transferred and concentrated to dryness at 35 °C. The dried residue was then re-dissolved in 1 mL of methanol by ultrasound. After centrifugation, again at 10,000 rpm for 10 min, the supernatant was transferred to an autosampler vial. Injection volumes were 5 and 1  $\mu$ L for RRLC-QqQ-MS and UHPLC-QE Orbitrap HRMS analysis, respectively.

### RRLC-QqQ-MS instrumentation and conditions

The RRLC-QqQ-MS system consisted of an RRLC system (Agilent Technologies, Palo Alto, CA, USA) including a G1311A binary pump, a G1311A vacuum degasser and G1311A autosampler, and triple quadrupole mass spectrometer equipped with an electrospray source (Series 6410, Agilent Technologies).

The analytes were separated on a Poroshell 120 SB-C18 column (100 mm  $\times$  4.6 mm; 2.7  $\mu$ m) and the column temperature was maintained at 25 °C. From 0 to 7 min, the A (water containing 0.1% (v/v) formic acid)/B (acetonitrile containing 0.1% (v/v) formic acid) was maintained at 25:75. From 7 to 17 min, the A was increased to 100%. From 17 to 20 min, the A was maintained at 100%. The total run time was 20 min.

The mobile phase was returned to the initial conditions and reequilibration was conducted for 10 min. The flow rate was 0.5 mL/min. The sample injection volume was 5  $\mu$ L.

The positive ion modes were performed with MRM for quantitative analysis by ESI. The MRM quantitative ions were then selected from the MS/MS data (see Electronic Supplementary Material (ESM) Table S1). The MS ionization source conditions were as follows: capillary voltage of 4.0 kV, drying gas temperature of 300 °C, drying gas flow rate of 11 L/min, corona current of 10 nA, and nebulizer pressure of 45 psi. The sheath gas temperature was 250 °C and sheath gas flow rate was 7 L/min.

### UHPLC-QE Orbitrap HRMS instrumentation and conditions

The metabolites analysis was performed using an UltiMate 3000 Hyperbaric LC system coupled to a Q Exactive MS. Chromatographic separation was performed using an Acquity UPLC CSH C18 column (1.7  $\mu$ m 100  $\times$  2.1 mm). Mobile phase A (water contained 2 mmol/L ammonium formate, *v/v*, 0.1% formic acid) and mobile phase B (methanol) were utilized at a flow rate of 0.4 mL/min. From 0 to 6 min, the A was increased to 100% from 25%. From 6 to 20 min, the A was maintained at 100%. Mobile phase gradient was as follows: the temperatures of the column oven and autosampler were set at 40 and 4 °C, respectively. The injection volume was 1  $\mu$ L.

The ESI source was operated in the positive mode with the following parameters: capillary temperature, 350 °C; source voltage and spray voltage, 3.7 kV; sheath gas (nitrogen) flow, 28 arb; and aux gas flow, 8 arb. Data were acquired using full MS scan (resolution, 70,000; AGC target,  $1 \times 10^6$ ; maximum IT, 120 ms; scan range, *m/z* 100–1500) and collision-induced dissociation (CID)-based data dependent on MS/MS (DDMS2) (resolution, 17,500; AGC target,  $1 \times 10^5$ ; maximum IT, 120 ms; loop count, 5; TopN = 5; isolation window, *m/z* 1.0; scan range, *m/z* 200–2000; NCE/stepped NCE: 30, 40, 50; underfill ratio, 1.0%; intensity threshold,  $1.0 \times 10^5$ ; apex trigger, 2–6 s; dynamic exclusion, 10 s).

### Preparation of calibration standards and quality control samples

The stock solutions of bergapten, narirutin, hesperidin, naringin, kaempferitrin, diosmin, diosmetin-7-O-glucoside, sinensetin, eriocitrin, neohesperidin, naringenin, hesperetin, luteolin, rutin, isopimpinellin, tangeretin, 5-demethylnobiletin, nobiletin, auraptene, rhoifolin, apigenin, apigenin-7-O-glucoside, scoparone, diosmetin, poncirin, limonin, nomilin, eriodictyol, xanthotoxol, acacetin, isosakuranetin, and imperatorin were separately dissolved in methanol to prepare a solution. A series of working standard

solutions were prepared by diluting the stock solution with 50% acetonitrile to obtain the following concentrations: 1, 2, 5, 10, 16, 80, 160, 320 ng/mL for acacetin; 2, 10, 20, 40, 60, 100, 400, 800 ng/mL for apigenin; 2, 6, 20, 50, 100, 500 1000, 4000 ng/mL for apigenin-7-O-glucoside; 1, 4, 10, 16, 40, 400, 1000, 2000 ng/mL for auraptene; 4, 8, 12, 24, 50, 100, 400, 800 ng/mL for bergapten; 5, 10, 30, 200, 2000, 20,000, 100,000, 500,000 ng/mL for 5-demethylnobiletin; 10, 20, 50, 100, 200, 1000, 10,000, 30,000 ng/mL for diosmetin; 20, 40, 100, 500, 1000, 5000, 10,000, 20,000 ng/mL for diosmetin-7-O-glucoside; 30, 90, 150, 300, 500, 30,000, 100,000, 300,000 ng/mL for diosmin; 20, 40, 60, 80, 400, 2000, 20,000, 300,000 ng/mL for eriocitrin; 10, 20, 50, 100, 200, 400, 800, 1000 ng/mL for eriodictyol; 200, 400, 600, 800, 1000, 10,000, 50,000, 100,000 ng/mL for hesperetin; 200, 400, 800, 2000, 10,000, 200,000, 4,000,000 ng/mL for hesperidin; 2, 4, 8, 10, 20, 40, 200, 400 ng/mL for imperatorin; 10, 20, 30, 60, 100, 400, 1000 ng/mL for isopimpinellin; 1, 2, 4, 8, 16, 160, 300, 600 ng/mL for isosakuranetin; 2, 4, 8, 16, 32, 500, 1000, 2000 ng/mL for kaempferitrin; 20, 40, 80, 100, 800, 4000, 10,000, 30,000 ng/mL for limonin; 20, 80, 200, 400, 800, 10,000, 80,000, 400,000 ng/mL for luteolin; 20, 40, 100, 200, 500, 5000, 20,000, 120,000 ng/mL for naringenin; 200, 400, 1000, 3000, 7000, 700,000, 7,000,000, 10,000,000 ng/mL for naringin; 50, 100, 500, 1000, 5000, 10,000, 100,000, 350,000 ng/mL for narirutin; 500, 1000, 5000, 10,000, 80,000, 800,000, 8,000,000, 16,000,000 ng/mL for neohesperidin; 20, 80, 200, 1000, 5000, 20,000, 200,000 2,500,000 ng/mL for nobiletin; 20, 40, 80, 100, 150, 1500, 5000, 15,000 ng/mL for nomilin; 6, 30, 60, 100, 800, 1600, 16,000, 160,000 ng/mL for poncirin; 10, 30, 60, 120, 2000, 20,000, 100,000, 500,000 ng/mL for rhoifolin; 6, 20, 40, 50, 500, 5000, 50,000, 500,000 ng/mL for rutin; 9, 20 40, 80, 100, 500, 1000, 6000 ng/mL for scoparone; 10, 20, 60, 100, 200, 1000, 50,000, 5,000,000 ng/mL for sinensetin; 15, 30, 60, 100, 1000, 10,000, 100,000, 1,000,000 ng/mL for tangeretin; 15, 30, 50, 60, 80, 160, 1600, 8000, 16,000 ng/mL for xanthotoxol. Quality control samples are at 1, 5, 10 ng/mL for acacetin; 2, 20, 40 ng/mL for apigenin; 2, 6, 20 ng/mL for apigenin-7-O-glucoside; 1, 10, 40 ng/mL for auraptene; 8, 12, 24 ng/mL for bergapten; 5, 10, 30 ng/mL for 5-demethylnobiletin; 20, 50, 200 ng/mL for diosmetin; 20, 100, 1000 ng/mL for diosmetin-7-O-glucoside; 30, 150, 500 ng/mL for diosmin; 20, 40, 80 ng/mL for eriocitrin; 10, 20, 50 ng/mL for eriodictyol; 200, 400, 800 ng/mL for hesperetin; 200, 800, 2000 ng/mL for hesperidin; 2, 4, 8 ng/mL for imperatorin; 10, 20, 30 ng/mL for isopimpinellin; 2, 8, 16 ng/mL for isosakuranetin; 4, 8, 16 ng/mL for kaempferitrin; 20, 100, 800 ng/mL for limonin; 20, 200, 800 ng/mL for luteolin; 20, 100, 500 ng/mL for naringenin; 200, 1000, 7000 ng/mL for naringin; 50, 500, 1000 ng/mL for narirutin; 500, 5000, 10,000 ng/mL for neohesperidin; 20, 200, 1000 ng/mL for nobiletin; 20, 80,

150 ng/mL for nomilin; 6, 30, 100 ng/mL for poncirin; 10, 60, 120 ng/mL for rhoifolin; 6, 20, 50 ng/mL for rutin; 9, 40, 80 ng/mL for scoparone; 10, 60, 200 ng/mL for sinensetin; 15, 60, 100 ng/mL for tangeretin; and 15, 50, 80 ng/mL for xanthotoxol. All solutions were stored at  $-20^{\circ}\text{C}$  before analysis.

## Method validation

### Selectivity

The selectivity of the method was evaluated by comparing the chromatograms of a blank plasma sample, a blank plasma sample spiked with the working solutions, the water extract of *Citrus* TCM, and a rat plasma sample after an oral administration of the water extract of *Citrus* TCM.

### Linearity and lower limit of quantification

The calibration curves of the tested compounds were determined by least-squares linear regression of the peak area versus the concentrations. Lower limit of quantification (LLOQ) is defined as the lowest level of the analytes that can be reliably quantified based on the signal-to-noise ratio of 10:1 and reproduced with a precision of less than 20% and an accuracy of 80–120%.

### Accuracy and precision

By analyzing six sets of quality control samples at three levels of concentration, the accuracy and accuracy (inter-day and intra-day) of the day were measured on 6 days with six concentrations on the same day or for three consecutive days. The accuracy was determined as RE (%) within the nominal value of 85–115%, the precision as RSD (%) within  $\pm 15\%$ , in addition to LLOQ, its accuracy should be within 80–120%, and cannot exceed 20% of precision.

### Recovery and matrix effect

Extraction recovery, evaluated in three replicates of QC sample, was determined by comparing the peak areas of extracted plasma (pre-spiked) standard QC samples to those of post-spiked standards at equivalent concentrations. The matrix effect was determined by comparing the peak response of the analytes in plasma samples with those of the pure standards prepared in the mobile phase. Six replicates of each concentration of quality control samples were prepared.

### Stability

The stability of the samples was evaluated by measuring the quality control samples' analysis data with freshly prepared

mass control samples at room temperature, frozen and freeze-thaw storage conditions. The short-term ( $25^{\circ}\text{C}$  for 4 h) and long-term ( $80^{\circ}\text{C}$  for 30 days) stabilities of the analytes were evaluated using the quality control samples at three concentrations. To assess the stability of the sample in the autosampler, the quality control sample was placed in the autosampler at room temperature for 24 h and then analyzed. The stability experiments were measured by analyzing replicates ( $n = 5$ ) during the sample storing and processing procedures.

## Statistical analysis

Quantitative data consisting of values taken from the RRLC-QqQ-MS analyses of the extract samples and plasma samples were used for the multivariate analysis. Multivariate statistical analyses, including analysis of variance through the formula:

$F = S_{\text{high}}^2/S_{\text{low}}^2$  and  $S^2 = \sum (X - \bar{X})^2/(n - 1)$  (calculate the  $F$  value and then compare with the  $F$  value table)

and Student's  $t$  test through the formula:

$$t = \frac{\bar{X}_1 - \bar{X}_2}{\sqrt{\frac{(n_1 - 1)S_1^2 + (n_2 - 1)S_2^2}{n_1 + n_2 - 2} \left( \frac{1}{n_1} + \frac{1}{n_2} \right)}}$$

were performed using SPSS 13.0.

## Results

### Method development.

#### Optimization of RRLC and QqQ-MS conditions

The plasma samples were precipitated with acetonitrile before RRLC-QqQ-MS analysis. The Poroshell 120 SB-C18 column has been proven to be suitable for simultaneous quantification of these analytes. The concentration of aqueous and organic 0.1% (v/v) formic acid solution was proved to give a better response than other aqueous phases and organic phases (e.g., for 0.2% formic acid). Gradient elution changed linearly from 25:75 (v/v) water containing 0.1% (v/v) formic acid-acetonitrile containing 0.1% (v/v) formic acid to 100:0 at a flow rate of 0.5 mL/min. The results showed that the best peak shape and resolution was obtained from a mixture of acetonitrile and water each containing 0.1% formic acid solution. The flow rate of 0.5 mL/min and column temperature of  $25^{\circ}\text{C}$  were demonstrated to be the most suitable. The established chromatographic conditions are listed in “RRLC-QqQ-MS instrumentation and conditions” section.

MRM patterns were superior to other models in targeted analysis, and MRM patterns were used to quantify the

analytes in rat plasma. The capillary temperature, the evaporator temperature, the flow rate of the analyte, and the fragmentation energy were optimized to obtain the protonated molecules and achieve the maximum response of the compound fragment ion peaks, and finding that the cationic mode provides better sensitivity for the target compound. Since the generated product ions are the most abundant, the use of MRM is used to simultaneously quantify 32 prototype analytes and to select quantitative ions.

#### Optimization of UHPLC and QE Orbitrap HRMS conditions

Different mobile phase compositions were screened to obtain LC chromatograms with better peak shape and separation. The water contained 2 mmol/L ammonium formate and 0.1% formic acid (v/v) in aqueous solution was ultimately selected as the mobile phase to obtain sufficiently good performance for these metabolites with good peak symmetry. To acquire better sensitivity for the base ions of most compounds in the QE Orbitrap HRMS spectra, the ionization parameters including capillary temperature, source voltage, spray voltage, sheath gas flow, and aux gas flow were optimized. The optimum conditions for QE Orbitrap HRMS were decided as follows: capillary temperature, 350 °C; source voltage and spray voltage, 3.7 kV; sheath gas (nitrogen) flow, 28 arb; and aux gas flow, 8 arb.

#### Targeted prototype drug metabolomics using RRLC-QqQ-MS analysis

##### Method validation

**Selectivity** Figure S1 in ESM shows the representative MRM chromatograms of the blank rat plasma (A), blank rat plasma spiked with 32 analytes (B), and an in vivo plasma sample obtained 1 h after oral administration (C). No endogenous or extraneous peaks interfering with the analytes at the retention time were observed, indicating the specificity of the method was acceptable.

**Linearity and lower limit of quantification** Representative calibration curves were as follows: acetaminophen:  $y = 0.0476x - 0.958$  ( $r = 0.999$ ), apigenin:  $y = 0.161x - 1.24$  ( $r = 0.998$ ), apigenin-7-O-glucoside:  $y = 0.155x - 8.51$  ( $r = 0.992$ ), auraptene:  $y = 0.0588x + 0.285$  ( $r = 0.998$ ), bergapten:  $y = 0.28x - 10.2$  ( $r = 0.991$ ), 5-demethylnobiletin:  $y = 0.0609x - 5.36$  ( $r = 0.990$ ), diosmetin:  $y = 0.132x - 3.63$  ( $r = 0.995$ ), diosmetin-7-O-glucoside:  $y = 0.908x - 9.68$  ( $r = 0.999$ ), diosmin:  $y = 1.04x + 0.528$  ( $r = 0.998$ ), eriocitrin:  $y = 0.813x - 3.64$  ( $r = 0.996$ ), eriodictyol:  $y = 0.565x + 2.42$  ( $r = 0.999$ ), hesperetin:  $y = 0.871x - 40.4$  ( $r = 0.999$ ), hesperidin:  $y = 0.565x - 2.61$  ( $r = 0.998$ ), imperatorin:  $y = 0.104x - 0.711$  ( $r = 0.991$ ), isopimpinellin:

$y = 0.0741x - 14.4$  ( $r = 0.999$ ), isosakuranetin:  $y = 0.214x - 9.05$  ( $r = 0.998$ ), kaempferitrin:  $y = 0.281x - 15.8$  ( $r = 0.998$ ), limonin:  $y = 1.56x + 1.05$  ( $r = 0.999$ ), luteolin:  $y = 0.703x - 12$  ( $r = 0.996$ ), naringenin:  $y = 0.374x - 24.5$  ( $r = 0.990$ ), naringin:  $y = 1.92x - 15.7$  ( $r = 0.995$ ), narirutin:  $y = 0.584x - 31.2$  ( $r = 0.999$ ), neohesperidin:  $y = 3.3x - 19.9$  ( $r = 0.999$ ), nobiletin:  $y = 0.0187x - 20.6$  ( $r = 0.993$ ), nomilin:  $y = 0.601x + 0.54$  ( $r = 0.992$ ), poncirin:  $y = 0.106x + 1.37$  ( $r = 0.998$ ), rhoifolin:  $y = 0.153x - 24.9$  ( $r = 0.998$ ), rutin:  $y = 0.432x + 2.38$  ( $r = 0.999$ ), scoparone:  $y = 0.177x - 20.3$  ( $r = 0.996$ ), sinensetin:  $y = 0.0396x - 2.63$  ( $r = 0.991$ ), tangeretin:  $y = 0.023x - 13.2$  ( $r = 0.997$ ), xanthotoxol:  $y = 0.163x - 0.365$  ( $r = 0.996$ ). The lowest concentrations with RSD <20% were taken as LLOQs and were found to be 0.8 ng/mL for acetaminophen, 1.3 ng/mL for apigenin, 1.6 ng/mL for apigenin-7-O-glucoside, 0.7 ng/mL for auraptene, 2.2 ng/mL for bergapten, 2.5 ng/mL for 5-demethylnobiletin, 5.3 ng/mL for diosmetin, 6.2 ng/mL for diosmetin-7-O-glucoside, 4.7 ng/mL for diosmin, 3.8 ng/mL for eriocitrin, 4.5 ng/mL for eriodictyol, 6.4 ng/mL for hesperetin, 10.6 ng/mL for hesperidin, 1.3 ng/mL for imperatorin, 3.3 ng/mL for isopimpinellin, 1.2 ng/mL for isosakuranetin, 2.1 ng/mL for kaempferitrin, 8.8 ng/mL for limonin, 7.6 ng/mL for luteolin, 6.8 ng/mL for naringenin, 12.6 ng/mL for naringin, 11.1 ng/mL for narirutin, 63.1 ng/mL for neohesperidin, 7.5 ng/mL for nobiletin, 7.1 ng/mL for nomilin, 2.7 ng/mL for poncirin, 3.4 ng/mL for rhoifolin, 3.8 ng/mL for rutin, 5.2 ng/mL for scoparone, 4.9 ng/mL for sinensetin, 7.9 ng/mL for tangeretin, and 4.8 ng/mL for xanthotoxol, respectively, which were sufficient for these studies.

**Accuracy and precision** Accuracy and intra- and inter-day precision of LLOQ and three quality control samples for the RRLC-QqQ-MS analysis are presented in Table 1. The accuracy data in the present study ranged from 85.7 to 114.5% (RE), and the intra- and inter-day precision were 5.1 to 14.6% and 3.0 to 14.8% (RSD). This indicated that the precision and accuracy of this method were acceptable.

**Extraction recovery and matrix effect** The mean recovery and matrix effect were analyzed by analyzing the three concentrations of the quality control sample five times for RRLC-QqQ-MS analysis. As detailed in Table 1, the mean recoveries of the analytes were between 86.9 and 110.9% (RSD <15%) and the corresponding matrix effect ranges from 87.1 to 111.5% (RSD <15%). Thus, it is shown that methanol is a viable and suitable medium for the extraction of analytes and that there is no measurable matrix effect on the ionization of the analyte.

**Sample stability** The stability of the quality control samples under different conditions at three concentrations was

**Table 1** The accuracy (intra- and inter-day), precision (intra- and inter-day), recovery, matrix effects, and stability for 32 compounds in rat plasma ( $n = 5$ )

| Compound                | Concentration (ng/mL) | Accuracy (%) ( $n = 5$ ) |           | Precision (RSD, %) ( $n = 5$ ) |           | Recovery (%) |               | Matrix Effects |               | Autosampler for 24 h |         | At -80 °C for 1 month |         | Freeze-thaw cycles |         |
|-------------------------|-----------------------|--------------------------|-----------|--------------------------------|-----------|--------------|---------------|----------------|---------------|----------------------|---------|-----------------------|---------|--------------------|---------|
|                         |                       | Intra-day                | Inter-day | Intra-day                      | Inter-day | Accuracy (%) | Precision (%) | Accuracy (%)   | Precision (%) | Mean (%)             | RSD (%) | Mean (%)              | RSD (%) | Mean (%)           | RSD (%) |
|                         |                       |                          |           |                                |           |              |               |                |               |                      |         |                       |         |                    |         |
| Acacetin                | 1                     | 95.1                     | 102.2     | 8.4                            | 11.9      | 105.4        | 7.5           | 107.9          | 3.6           | 95.2                 | 3.1     | 101.1                 | 9.5     | 97.2               | 7.6     |
|                         | 5                     | 106.4                    | 101.2     | 6.7                            | 5.3       | 99.4         | 5.7           | 99.1           | 6.5           | 97.3                 | 3.6     | 100.9                 | 7.7     | 100.5              | 6.5     |
|                         | 10                    | 85.7                     | 86.4      | 11.3                           | 11.9      | 93.0         | 4.8           | 89.0           | 3.5           | 95.7                 | 3.3     | 96.2                  | 7.9     | 101.1              | 3.9     |
| Apigenin                | 2                     | 91.2                     | 112.8     | 12.3                           | 12.8      | 102.5        | 6.9           | 91.6           | 6.8           | 97.6                 | 3.5     | 100.9                 | 4.6     | 95.5               | 7.9     |
|                         | 20                    | 114.5                    | 94.7      | 14.6                           | 14.0      | 91.3         | 8.5           | 104.2          | 4.7           | 97.4                 | 3.4     | 97.2                  | 9.9     | 98.8               | 4.6     |
|                         | 40                    | 97.6                     | 100.6     | 13.6                           | 14.3      | 106.5        | 6.8           | 106.3          | 5.9           | 101.8                | 9.4     | 100.1                 | 3.9     | 99.9               | 9.1     |
| Apigenin-7-O-glucoside  | 2                     | 109.8                    | 96.2      | 10.2                           | 8.3       | 99.9         | 4.9           | 101.5          | 3.9           | 100.4                | 5.2     | 100.2                 | 7.0     | 99.3               | 9.4     |
|                         | 20                    | 112.4                    | 91.4      | 10.0                           | 12.5      | 107.4        | 5.3           | 97.9           | 7.5           | 99.6                 | 4.6     | 96.8                  | 6.2     | 96.2               | 6.8     |
|                         | 50                    | 94.1                     | 97.9      | 13.4                           | 11.7      | 106.5        | 7.1           | 102.3          | 9.4           | 98.7                 | 7.4     | 97.3                  | 3.0     | 96.0               | 9.0     |
| Auraptene               | 1                     | 102.9                    | 93.8      | 13.6                           | 10.5      | 93.7         | 5.1           | 102.5          | 6.5           | 95.9                 | 8.2     | 97.1                  | 8.0     | 99.5               | 6.0     |
|                         | 10                    | 102.8                    | 85.8      | 8.8                            | 5.5       | 108.0        | 9.4           | 94.3           | 7.4           | 99.5                 | 8.1     | 99.4                  | 9.2     | 98.4               | 9.1     |
|                         | 40                    | 90.2                     | 95.9      | 10.0                           | 5.8       | 86.9         | 9.0           | 102.7          | 10.9          | 100.5                | 4.4     | 96.4                  | 6.9     | 101.7              | 9.1     |
| Bergapten               | 8                     | 106.0                    | 90.4      | 10.8                           | 6.1       | 107.2        | 10.5          | 90.8           | 4.6           | 96.0                 | 5.5     | 98.0                  | 9.6     | 95.4               | 7.8     |
|                         | 12                    | 103.4                    | 100.0     | 9.9                            | 11.6      | 104.5        | 9.5           | 108.8          | 6.8           | 95.9                 | 3.4     | 101.3                 | 8.8     | 100.7              | 6.8     |
|                         | 24                    | 103.7                    | 109.3     | 7.9                            | 11.1      | 106.4        | 8.4           | 94.4           | 8.9           | 100.9                | 6.1     | 100.0                 | 7.3     | 101.0              | 10.0    |
| 5-Demethylnobiletin     | 5                     | 106.2                    | 89.1      | 11.2                           | 9.6       | 94.2         | 6.1           | 107.7          | 9.2           | 98.0                 | 8.4     | 98.5                  | 7.1     | 100.4              | 9.5     |
|                         | 10                    | 109.2                    | 108.2     | 12.5                           | 13.6      | 95.3         | 4.3           | 87.6           | 4.0           | 96.1                 | 8.4     | 101.5                 | 3.9     | 99.9               | 5.2     |
|                         | 30                    | 87.0                     | 99.7      | 12.7                           | 13.2      | 102.1        | 8.2           | 102.8          | 8.7           | 100.2                | 5.7     | 98.4                  | 9.1     | 97.7               | 3.8     |
| Diosmetin               | 20                    | 104.0                    | 111.4     | 7.4                            | 12.6      | 102.8        | 8.6           | 98.7           | 4.8           | 95.5                 | 5.0     | 97.1                  | 3.3     | 99.6               | 6.0     |
|                         | 50                    | 89.6                     | 106.4     | 7.3                            | 10.6      | 105.4        | 9.6           | 93.9           | 9.1           | 100.7                | 6.7     | 96.0                  | 3.8     | 100.9              | 10.0    |
|                         | 200                   | 98.8                     | 92.7      | 10.9                           | 13.6      | 88.0         | 8.7           | 104.5          | 7.1           | 101.1                | 10.0    | 101.4                 | 6.7     | 95.3               | 5.3     |
| Diosmetin-7-O-glucoside | 20                    | 86.6                     | 86.7      | 9.8                            | 6.5       | 98.9         | 7.7           | 103.2          | 7.0           | 100.5                | 6.1     | 101.1                 | 3.0     | 99.1               | 6.2     |
|                         | 100                   | 112.2                    | 102.0     | 12.6                           | 3.0       | 94.3         | 4.1           | 105.5          | 9.1           | 99.9                 | 9.5     | 99.1                  | 4.0     | 100.5              | 3.3     |
|                         | 1000                  | 111.0                    | 96.2      | 11.7                           | 11.7      | 101.3        | 4.0           | 91.3           | 10.8          | 100.1                | 4.5     | 99.2                  | 5.0     | 100.8              | 4.6     |
| Diosmin                 | 30                    | 93.3                     | 92.0      | 6.4                            | 13.6      | 103.6        | 10.3          | 91.3           | 7.5           | 97.1                 | 8.5     | 98.1                  | 4.9     | 100.2              | 7.2     |
|                         | 150                   | 97.2                     | 107.5     | 12.2                           | 14.5      | 94.9         | 5.9           | 104.0          | 4.4           | 97.8                 | 7.9     | 95.3                  | 6.5     | 98.7               | 9.7     |
|                         | 500                   | 96.0                     | 91.1      | 9.3                            | 12.3      | 100.8        | 3.9           | 106.5          | 9.5           | 100.9                | 9.4     | 100.6                 | 7.2     | 99.6               | 7.3     |
| Eriocitrin              | 20                    | 91.9                     | 109.1     | 6.3                            | 9.3       | 110.4        | 8.6           | 88.8           | 3.7           | 96.8                 | 4.8     | 99.1                  | 5.8     | 99.7               | 5.2     |
|                         | 40                    | 99.3                     | 90.5      | 9.2                            | 10.4      | 91.0         | 7.4           | 101.5          | 9.4           | 101.6                | 5.6     | 96.8                  | 9.5     | 97.5               | 4.4     |
|                         | 80                    | 113.9                    | 92.0      | 10.7                           | 14.8      | 104.7        | 10.4          | 95.7           | 6.9           | 101.3                | 9.7     | 98.2                  | 5.1     | 97.5               | 7.3     |
| Eriodictyol             | 10                    | 94.0                     | 113.6     | 10.1                           | 9.3       | 87.2         | 8.3           | 103.8          | 9.1           | 100.5                | 6.3     | 99.6                  | 6.8     | 95.8               | 7.4     |
|                         | 20                    | 103.6                    | 87.5      | 5.4                            | 6.4       | 88.2         | 9.2           | 110.4          | 6.9           | 100.1                | 4.8     | 101.3                 | 9.0     | 96.9               | 7.6     |

Table 1 (continued)

| Compound       | Concentration (ng/mL) | Accuracy (%)     |           | Precision (RSD, %) |           | Recovery     |               | Matrix Effects |               | Autosampler for 24 h |         | At -80 °C for 1 month |         | Freeze-thaw cycles |         |          |         |
|----------------|-----------------------|------------------|-----------|--------------------|-----------|--------------|---------------|----------------|---------------|----------------------|---------|-----------------------|---------|--------------------|---------|----------|---------|
|                |                       | Accuracy (n = 5) |           | Precision (n = 5)  |           | Accuracy (%) |               | Precision (%)  |               | Mean (%)             |         | RSD (%)               |         | Mean (%)           |         | RSD (%)  |         |
|                |                       | Intra-day        | Inter-day | Intra-day          | Inter-day | Accuracy (%) | Precision (%) | Accuracy (%)   | Precision (%) | Mean (%)             | RSD (%) | Mean (%)              | RSD (%) | Mean (%)           | RSD (%) | Mean (%) | RSD (%) |
| Hesperetin     | 50                    | 111.5            | 90.4      | 9.2                | 12.5      | 92.9         | 10.5          | 102.3          | 4.6           | 96.4                 | 9.8     | 8.7                   | 96.4    | 8.7                | 97.3    | 3.9      |         |
|                | 200                   | 105.0            | 102.4     | 10.7               | 5.7       | 101.5        | 5.6           | 106.5          | 4.8           | 100.9                | 9.0     | 5.7                   | 99.7    | 5.7                | 98.0    | 3.1      |         |
|                | 400                   | 94.8             | 106.4     | 11.6               | 5.6       | 94.3         | 6.1           | 103.0          | 11.0          | 99.9                 | 9.2     | 5.7                   | 95.1    | 5.7                | 97.1    | 7.8      |         |
|                | 800                   | 113.8            | 105.7     | 8.4                | 12.1      | 107.5        | 6.7           | 96.7           | 7.3           | 99.5                 | 6.5     | 8.9                   | 96.4    | 8.9                | 99.4    | 7.2      |         |
| Hesperidin     | 200                   | 101.7            | 107.2     | 11.4               | 9.5       | 103.9        | 3.4           | 87.1           | 4.4           | 98.8                 | 3.9     | 6.1                   | 95.6    | 6.1                | 97.6    | 7.2      |         |
|                | 800                   | 96.9             | 97.6      | 8.1                | 7.3       | 93.5         | 4.3           | 101.0          | 10.5          | 100.2                | 3.2     | 6.9                   | 95.3    | 6.9                | 100.8   | 9.1      |         |
|                | 2000                  | 97.4             | 89.0      | 7.3                | 12.3      | 99.8         | 6.8           | 104.0          | 6.2           | 99.0                 | 6.1     | 7.0                   | 95.2    | 7.0                | 98.9    | 8.4      |         |
|                | 2                     | 109.4            | 103.4     | 7.1                | 7.9       | 99.5         | 7.9           | 85.3           | 8.3           | 100.6                | 7.4     | 6.3                   | 96.9    | 6.3                | 96.7    | 3.2      |         |
| Imperatorin    | 4                     | 96.2             | 87.9      | 10.7               | 10.3      | 109.9        | 5.5           | 108.5          | 9.5           | 98.1                 | 8.9     | 9.2                   | 96.7    | 9.2                | 100.4   | 6.9      |         |
|                | 8                     | 111.1            | 95.2      | 8.0                | 13.0      | 87.6         | 9.1           | 93.1           | 9.9           | 98.8                 | 6.4     | 3.6                   | 96.1    | 3.6                | 98.0    | 8.9      |         |
|                | 10                    | 112.1            | 99.1      | 14.6               | 12.9      | 90.8         | 10.8          | 105.2          | 9.4           | 101.3                | 4.4     | 3.2                   | 98.2    | 3.2                | 101.8   | 9.2      |         |
|                | 20                    | 86.2             | 105.6     | 10.9               | 5.6       | 98.5         | 8.7           | 100.3          | 6.2           | 95.9                 | 4.1     | 5.9                   | 95.9    | 5.9                | 97.0    | 5.4      |         |
| Isosakuranetin | 30                    | 94.2             | 106.0     | 8.0                | 5.9       | 106.3        | 8.8           | 108.3          | 5.2           | 99.1                 | 6.4     | 4.6                   | 101.3   | 4.6                | 98.4    | 5.3      |         |
|                | 2                     | 88.2             | 96.5      | 12.4               | 14.3      | 102.4        | 9.5           | 111.2          | 9.2           | 95.1                 | 8.5     | 7.1                   | 98.7    | 7.1                | 100.5   | 3.2      |         |
|                | 8                     | 104.0            | 95.4      | 7.2                | 11.8      | 108.2        | 8.7           | 97.9           | 10.1          | 96.3                 | 4.3     | 4.3                   | 97.2    | 4.3                | 95.9    | 4.1      |         |
|                | 16                    | 92.9             | 92.8      | 8.8                | 5.1       | 93.8         | 10.3          | 94.8           | 3.4           | 98.5                 | 5.0     | 5.7                   | 97.8    | 5.7                | 97.8    | 7.1      |         |
| Kaempferitin   | 4                     | 108.0            | 106.5     | 13.4               | 12.5      | 103.7        | 9.8           | 104.0          | 6.9           | 101.0                | 7.5     | 7.3                   | 95.2    | 7.3                | 99.4    | 6.2      |         |
|                | 8                     | 88.7             | 104.2     | 5.5                | 13.1      | 106.8        | 3.9           | 86.2           | 5.4           | 99.9                 | 7.0     | 7.0                   | 101.1   | 7.0                | 97.7    | 3.8      |         |
|                | 16                    | 108.5            | 89.4      | 7.5                | 7.6       | 99.6         | 7.4           | 103.1          | 5.0           | 96.3                 | 8.3     | 4.5                   | 99.0    | 4.5                | 101.5   | 8.7      |         |
|                | 20                    | 93.6             | 85.5      | 7.8                | 3.4       | 87.3         | 4.6           | 93.2           | 7.5           | 95.2                 | 4.1     | 6.2                   | 98.0    | 6.2                | 100.0   | 9.4      |         |
| Limonin        | 100                   | 103.4            | 85.9      | 7.3                | 5.5       | 88.2         | 6.2           | 105.9          | 9.6           | 96.1                 | 9.0     | 9.7                   | 99.6    | 9.7                | 100.6   | 5.3      |         |
|                | 800                   | 103.3            | 98.3      | 8.6                | 5.8       | 98.8         | 6.5           | 89.1           | 3.5           | 99.8                 | 6.8     | 7.3                   | 97.4    | 7.3                | 99.5    | 6.2      |         |
|                | 20                    | 104.4            | 110.2     | 14.6               | 14.4      | 95.5         | 9.5           | 90.9           | 4.5           | 97.9                 | 4.2     | 6.3                   | 100.2   | 6.3                | 97.9    | 6.0      |         |
|                | 200                   | 98.1             | 101.9     | 9.5                | 6.8       | 88.0         | 7.1           | 111.5          | 5.2           | 96.9                 | 4.1     | 7.1                   | 95.9    | 7.1                | 95.3    | 3.5      |         |
| Naringenin     | 800                   | 103.7            | 114.9     | 13.9               | 12.7      | 107.0        | 7.1           | 104.1          | 8.9           | 100.5                | 9.1     | 4.9                   | 98.7    | 4.9                | 101.8   | 3.1      |         |
|                | 20                    | 92.0             | 102.5     | 5.5                | 6.3       | 94.1         | 4.5           | 97.7           | 7.2           | 96.5                 | 8.5     | 8.5                   | 100.3   | 8.5                | 97.5    | 7.1      |         |
|                | 100                   | 95.1             | 85.5      | 10.3               | 10.9      | 110.6        | 7.4           | 107.2          | 8.8           | 96.3                 | 5.9     | 9.3                   | 95.1    | 9.3                | 98.8    | 5.8      |         |
|                | 500                   | 109.2            | 85.8      | 12.7               | 7.4       | 108.1        | 8.5           | 109.5          | 5.6           | 101.6                | 4.7     | 7.0                   | 100.0   | 7.0                | 99.6    | 9.6      |         |
| Naringin       | 200                   | 95.0             | 112.1     | 5.9                | 13.2      | 104.2        | 3.6           | 89.1           | 9.3           | 99.7                 | 8.0     | 8.7                   | 97.6    | 8.7                | 97.4    | 5.1      |         |
|                | 1000                  | 102.6            | 95.3      | 6.9                | 6.2       | 89.0         | 3.1           | 103.4          | 6.6           | 101.5                | 9.1     | 5.0                   | 98.2    | 5.0                | 96.2    | 9.9      |         |
|                | 7000                  | 107.7            | 106.7     | 13.6               | 13.5      | 93.0         | 9.7           | 109.6          | 5.0           | 101.0                | 4.6     | 7.4                   | 96.3    | 7.4                | 96.3    | 9.0      |         |
|                | 50                    | 92.7             | 100.8     | 6.6                | 12.7      | 89.1         | 3.3           | 99.3           | 5.0           | 100.9                | 9.5     | 10.0                  | 101.8   | 10.0               | 97.4    | 7.8      |         |



**Table 1** (continued)

| Compound      | Concentration (ng/mL) | Accuracy (%)     |           | Precision (RSD, %) Recovery |           | Matrix Effects |               | Autosampler for 24 h |         | At -80 °C for 1 month |         | Freeze-thaw cycles |         |       |      |
|---------------|-----------------------|------------------|-----------|-----------------------------|-----------|----------------|---------------|----------------------|---------|-----------------------|---------|--------------------|---------|-------|------|
|               |                       | Accuracy (n = 5) |           | Precision (n = 5)           |           | Accuracy (%)   |               | Precision (%)        |         | Mean (%)              |         | RSD (%)            |         |       |      |
|               |                       | Intra-day        | Inter-day | Intra-day                   | Inter-day | Accuracy (%)   | Precision (%) | Mean (%)             | RSD (%) | Mean (%)              | RSD (%) | Mean (%)           | RSD (%) |       |      |
| Neohesperidin | 500                   | 89.4             | 114.3     | 12.1                        | 10.7      | 104.6          | 10.6          | 96.8                 | 9.0     | 99.4                  | 7.4     | 96.7               | 8.9     | 100.9 | 7.0  |
|               | 1000                  | 89.1             | 113.0     | 13.3                        | 14.6      | 88.5           | 8.3           | 98.8                 | 8.6     | 101.9                 | 4.0     | 98.3               | 9.1     | 98.3  | 10.0 |
|               | 500                   | 114.3            | 105.3     | 6.1                         | 5.8       | 110.4          | 5.6           | 95.1                 | 10.6    | 102.0                 | 6.9     | 97.4               | 3.9     | 99.0  | 7.0  |
|               | 5000                  | 94.2             | 97.3      | 6.9                         | 10.9      | 93.5           | 5.0           | 104.7                | 10.3    | 95.2                  | 9.8     | 99.5               | 7.6     | 95.9  | 5.5  |
|               | 10,000                | 89.3             | 87.2      | 13.7                        | 8.7       | 105.4          | 4.1           | 90.8                 | 9.4     | 98.8                  | 7.9     | 101.7              | 8.0     | 101.9 | 6.6  |
| Nobiletin     | 20                    | 88.0             | 90.4      | 9.3                         | 14.8      | 109.6          | 9.9           | 94.5                 | 10.2    | 99.9                  | 7.5     | 95.3               | 3.3     | 98.6  | 5.1  |
|               | 200                   | 114.3            | 102.1     | 8.3                         | 9.2       | 106.3          | 7.0           | 88.1                 | 3.9     | 96.5                  | 8.7     | 97.3               | 6.1     | 98.2  | 8.5  |
|               | 1000                  | 87.9             | 99.3      | 8.1                         | 6.4       | 102.9          | 5.1           | 109.5                | 3.5     | 99.9                  | 5.3     | 101.8              | 4.0     | 97.4  | 6.8  |
| Nominin       | 20                    | 104.7            | 97.9      | 14.1                        | 7.8       | 106.2          | 6.2           | 108.2                | 11.0    | 96.3                  | 7.9     | 97.4               | 4.0     | 97.4  | 3.2  |
|               | 80                    | 93.8             | 97.5      | 9.1                         | 11.5      | 107.6          | 4.9           | 93.0                 | 3.6     | 97.2                  | 5.6     | 99.8               | 8.3     | 101.6 | 8.7  |
|               | 150                   | 95.4             | 107.2     | 11.5                        | 7.4       | 91.0           | 6.2           | 106.1                | 3.1     | 98.8                  | 5.1     | 100.9              | 9.1     | 101.1 | 5.5  |
| Poncirin      | 6                     | 104.8            | 89.5      | 8.2                         | 9.2       | 93.9           | 3.2           | 95.8                 | 5.8     | 101.8                 | 8.3     | 99.1               | 6.9     | 97.6  | 5.6  |
|               | 30                    | 86.6             | 88.2      | 7.4                         | 5.8       | 103.7          | 9.3           | 94.0                 | 4.9     | 96.3                  | 9.6     | 95.2               | 8.1     | 96.3  | 5.1  |
|               | 100                   | 95.4             | 106.5     | 12.2                        | 8.7       | 91.7           | 8.7           | 92.3                 | 4.5     | 99.8                  | 4.3     | 96.3               | 5.0     | 97.2  | 7.7  |
| Rhoifolin     | 10                    | 114.0            | 106.6     | 6.3                         | 5.3       | 89.1           | 9.5           | 105.3                | 10.7    | 97.2                  | 3.6     | 100.7              | 5.8     | 95.9  | 3.1  |
|               | 60                    | 104.2            | 107.7     | 10.3                        | 7.5       | 103.6          | 7.4           | 107.9                | 3.9     | 99.6                  | 4.1     | 97.0               | 5.7     | 96.6  | 6.5  |
|               | 120                   | 109.5            | 103.6     | 6.4                         | 14.7      | 87.9           | 3.7           | 109.3                | 6.2     | 100.6                 | 7.1     | 100.4              | 7.7     | 98.3  | 5.0  |
| Rutin         | 6                     | 94.2             | 88.5      | 14.1                        | 13.8      | 107.5          | 4.0           | 91.3                 | 3.3     | 97.5                  | 6.3     | 98.0               | 5.0     | 101.6 | 5.5  |
|               | 20                    | 104.5            | 97.0      | 9.1                         | 8.6       | 110.9          | 10.5          | 107.2                | 10.7    | 95.2                  | 7.7     | 100.4              | 8.4     | 95.5  | 4.3  |
|               | 50                    | 114.2            | 95.3      | 8.2                         | 12.4      | 97.5           | 4.1           | 110.7                | 4.5     | 101.7                 | 10.0    | 97.0               | 3.2     | 101.7 | 8.4  |
| Scoparone     | 9                     | 96.4             | 99.5      | 8.7                         | 13.8      | 102.0          | 7.5           | 109.5                | 10.5    | 98.5                  | 7.7     | 96.7               | 7.6     | 99.8  | 8.1  |
|               | 40                    | 109.2            | 88.9      | 5.8                         | 8.5       | 95.4           | 7.4           | 93.5                 | 3.1     | 98.7                  | 3.4     | 100.7              | 4.5     | 100.9 | 9.3  |
|               | 80                    | 103.7            | 110.2     | 10.5                        | 11.0      | 109.3          | 5.6           | 108.2                | 4.6     | 96.6                  | 5.2     | 100.9              | 6.2     | 101.2 | 4.4  |
| Sinensetin    | 10                    | 102.4            | 108.1     | 10.4                        | 8.7       | 87.5           | 6.7           | 92.5                 | 9.1     | 97.9                  | 4.3     | 101.3              | 7.5     | 101.0 | 9.1  |
|               | 60                    | 96.0             | 89.4      | 7.8                         | 8.1       | 103.0          | 3.7           | 92.6                 | 3.5     | 101.1                 | 5.8     | 100.3              | 4.0     | 100.5 | 3.5  |
|               | 200                   | 111.0            | 103.6     | 7.7                         | 9.1       | 103.8          | 10.8          | 105.7                | 9.8     | 96.7                  | 3.6     | 99.1               | 8.4     | 96.2  | 5.6  |
| Tangeretin    | 15                    | 106.4            | 99.2      | 6.0                         | 7.2       | 107.3          | 4.8           | 87.2                 | 5.7     | 96.6                  | 5.2     | 99.9               | 6.3     | 99.6  | 5.8  |
|               | 60                    | 113.8            | 87.4      | 12.5                        | 11.0      | 100.6          | 3.7           | 108.0                | 5.0     | 96.0                  | 8.7     | 96.3               | 6.6     | 101.3 | 3.6  |
|               | 100                   | 108.0            | 113.4     | 6.7                         | 9.9       | 99.5           | 3.3           | 109.0                | 6.9     | 101.6                 | 4.2     | 97.8               | 3.6     | 96.0  | 4.6  |
| Xanthoxol     | 15                    | 85.9             | 104.6     | 9.7                         | 7.4       | 103.5          | 3.9           | 102.1                | 5.5     | 98.4                  | 4.2     | 101.9              | 5.8     | 95.1  | 6.8  |
|               | 50                    | 92.2             | 113.3     | 9.2                         | 6.8       | 107.5          | 6.3           | 108.8                | 7.3     | 101.7                 | 8.6     | 96.0               | 9.3     | 101.4 | 3.5  |
|               | 80                    | 106.7            | 87.9      | 10.2                        | 6.7       | 96.8           | 3.7           | 96.3                 | 3.5     | 97.5                  | 8.3     | 100.0              | 5.8     | 99.2  | 3.7  |

evaluated using the newly prepared mass control samples' peak area. The results are presented in Table 1. The results indicated that these analytes were all stable in rat plasma with accuracy in the range from 95.1 to 102.0% after 24 h in the room temperature (20 °C), storage at -80 °C for 1 month, and three freeze-thaw cycles.

#### *Quantification of plasma pharmacochemistry targeted to 32 prototypical constituents*

It is well-known that the effects of TCMs are produced by their chemical constituents, and it is also accepted that only compounds absorbed into the blood have the opportunity to show bioactivity according to the opinion of plasma pharmacochemistry. In the present study, a developed quantitative plasma pharmacochemistry method was established to assist in the selection of reasonable QC-markers based on the absorption of prototypical compounds. Plant metabolomics is the profiling of the complete set of small-molecule metabolites, such as metabolic intermediates, hormones, and other signaling molecules, as well as secondary metabolites [7]. Plant metabolomics is an efficient analytical method that can aid in the understanding of the mechanisms/modes of the biosynthesis of secondary metabolites and in the identification of potential chemotaxonomic markers of different TCMs. In our recent study, a total of 73 active secondary metabolites were identified as potential classification markers among four *Citrus* TCMs using a plant metabolomics method. Among them, 32 chemotaxonomic markers were quantitatively determined and validated to be characteristic of the specific TCMs.

In this study, the targeted 32 prototypical compounds, including 11 glycosides, 9 flavonoids, 6 coumarins, 4 flavanones, and 2 limonoids, which are characteristically [8] and bioactively [2, 9–11] present in the four *Citrus* TCMs, were determined in these 4 standard vehicles and 28 biological samples after oral administration (eight samples each). Representative MRM chromatograms are shown in Fig. 1. The calibration curves were used for the quantitative determination of the 32 compounds. The contents of the 32 prototypical compounds in four *Citrus* standard vehicles and biological samples were then measured and are shown in ESM Table S2.

#### *Comparison of the relative prototypical absorption among different vehicle matrices*

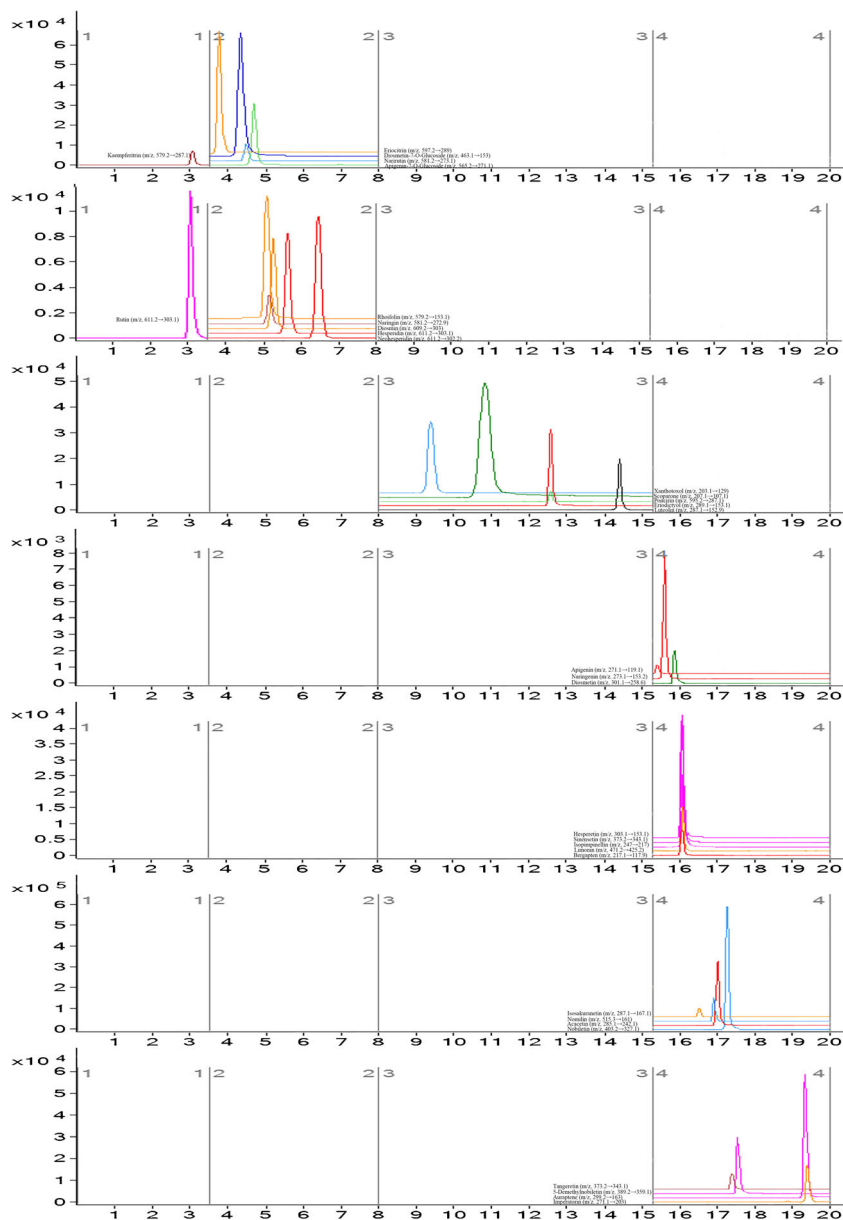
Based on the results depicted in Fig. 2, the changes in absorption of the prototypical constituents correspond with the method of quantitative plasma pharmacochemistry, which are presented in the box-plot with different colors. The potential correlations were analyzed between the in vitro standard vehicle matrix and in vivo blood samples of prototype constituents. The statistical analyses that are used to calculate correlations

between treatment groups and *Citrus* standard vehicles, such as Student's *t* test and Fisher ratios (common approaches for identifying putative variant prototype constituents), are reliant upon contents of prototypical compounds. Analysis by Student's *t* test was employed to determine significant differences between each of the four *Citrus* standard vehicles and biological samples. Subsequently, the between-group vs. within-group variance of each compound was assessed in the biological samples where the compounds with higher Fisher ratios were regarded as potential candidate markers.

The result showed that 14 varied prototypical constituents were completely different from the normal level after oral administration with Zhiqiao extracts. Some of these showed relatively higher absorption, including apigenin, eriodictyol, nomilin, diosmetin-7-O-glucoside, hesperetin, naringenin, diosmin, and diosmetin. Certainly, some exhibited relatively lower absorption, including rhoifolin, apigenin-7-O-glucoside, nobiletin, tangeretin, 5-demethylnobiletin, and sinensetin. The treatment of the Zhishi extracts group showed relatively higher absorption in eriodictyol, xanthotoxol, diosmetin-7-O-glucoside, hesperetin, naringenin, and luteolin and relatively lower absorption in nobiletin, tangeretin, 5-demethylnobiletin, and sinensetin. The obvious changes in the group with Qingpi treatment included significantly higher absorption of scoparone, nomlin, limonin, diosmetin-7-O-glucoside, hesperetin, and naringenin, accompanied by significantly lower absorption of naringin, nobiletin, tangeretin, 5-demethylnobiletin, and sinensetin. Meanwhile, significant differences were observed with the group given oral medication Chenpi extracts, and the absorption of eriodictyol, nomilin, diosimin, limonin, and hesperetin was relatively higher and the absorption of nobiletin, tangeretin, 5-demethylnobiletin, and sinensetin was relatively lower.

#### **Metabolite identification and biotransformation**

Metabolites of prototypical compounds in four *Citrus* TCMs were identified using Progenesis QI software which contains multiple MS identification tools, including MS fragmentation scan, spectra matching, fragment ion annotation, and elemental composition prediction. To identify every screened metabolite rapidly, effectively, and accurately, great efforts were made for metabolite identification, which included isotopic characteristic fragment ion recognition (CFIR), constant neutral loss filtering (CNLF), pattern recognition (IPR), and mass defect filtering (MDF). Most of the prototypical compounds in the four *Citrus* TCMs and their metabolites contain benzene rings; thus, the CNLF method can indirectly predict biotransformation that occurs on the ring. It was found that phase I metabolites had characteristic neutral loss on the benzene ring, especially for the loss of H<sub>2</sub>O/H<sub>2</sub>O<sub>2</sub> (for hydroxylated metabolites, e.g., M9-M11, M14-M16, M20, M21, M24-M26, M37, M48-M50, and M65) and CH<sub>3</sub>OH/CH<sub>2</sub>O (for the

**Fig. 1** MRM figure for 32 compounds in four *Citrus* TCMs

methoxylated metabolites, e.g., M29, M33, M34, and M38). The screened phase II metabolites included conjugates of glucuronide (M22, M39, M44, M51, and M52) and sulfate (M4, M12, M23, M30, M40, M43, and M53), predominantly presenting their specific fragments related to neutral loss of Glu moiety (176.0321 Da, <4 ppm, M22, M39, M44, M51, and M52), SO<sub>3</sub> moiety (79.9563 Da, <4 ppm, M4, M12, M23, M30, M40, M43, and M53), and sulfate and glucuronide moiety (255.9889 Da, <4 ppm, M19 and M54), respectively. These results were consistent with previous studies [12, 13]. In the MS ionization process, because of the high stability of benzene ring, CFIR can be used to predict the corresponding metabolites, which include preliminary identification of readily identifiable metabolites to enrich the annotation of the corresponding fragment ions.

#### Hydroxylated and dehydroxylated metabolites

Metabolites M1 ( $t_R$  8.873 min), M3 ( $t_R$  8.898 min), M6 ( $t_R$  8.651 min), M31 ( $t_R$  8.667 min), M36 ( $t_R$  8.752 min), M45 ( $t_R$  8.805 min), and M56 ( $t_R$  8.674 min) had the formula C<sub>15</sub>H<sub>12</sub>O<sub>7</sub>, C<sub>16</sub>H<sub>12</sub>O<sub>7</sub>, C<sub>15</sub>H<sub>10</sub>O<sub>6</sub>, C<sub>15</sub>H<sub>10</sub>O<sub>6</sub>, C<sub>11</sub>H<sub>6</sub>O<sub>5</sub>, C<sub>21</sub>H<sub>22</sub>O<sub>9</sub>, and C<sub>20</sub>H<sub>20</sub>O<sub>9</sub> for the [M + H]<sup>+</sup> ions shown in Table 2, which were approximately 16 Da (+ O) or 32 Da (+ 2O) higher than eriodictyol, diosmetin, apigenin, xanthotoxol, nobiletin, and 5-demethylnobiletin, suggesting that the metabolite may be formed by the hydroxylate of prototypical compounds. For M2, M7, M8, M17, M18, M27, M28, M32, M35, M41, M42, M59, M61, M63, and M64, as shown in Table 2, had ions  $m/z$  369.1805, 285.1595, 257.0834, 269.1756, 253.1807, 261.1132, 261.1131, 256.1035, 256.1206,

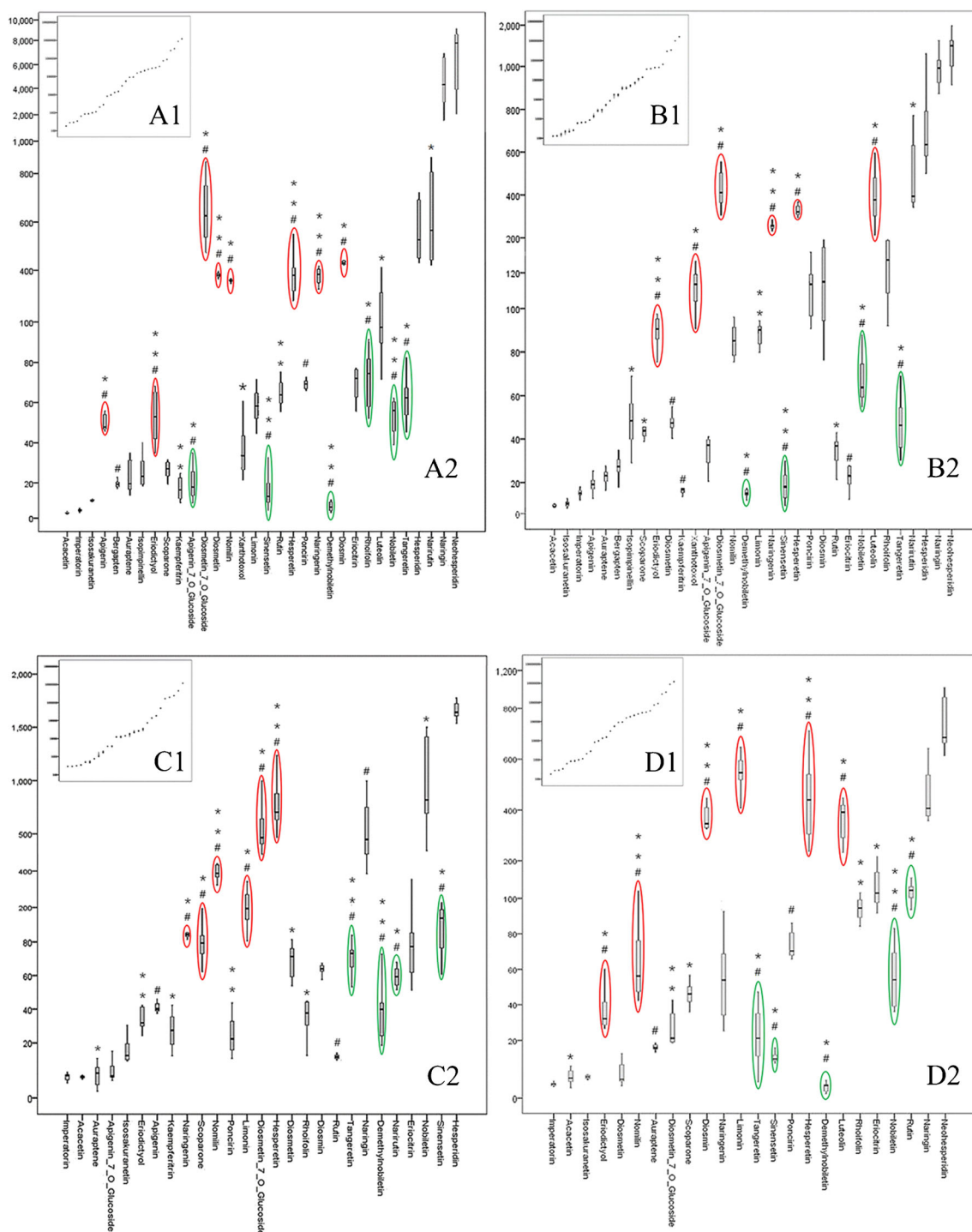


**Fig. 2** Combined box-and-whisker and dot plot of quantitative content of 32 prototypical compounds in Zhiqiao, Zhishi, Qingpi, and Chengpi groups (A1, B1, C1, and D1 for the *Citrus* TCMs extracts; A2, B2, C2, and D2 for plasma sample). The order of the prototypical compounds is arranged in descending order according to the content of the compound in the *Citrus* TCMs extracts, and the thumbnail (A1, B1, C1, and D1) is the same order as the A2, B2, C2, and D2. The potential candidate markers of

relative higher absorption were marked by *red circle*, and the markers of relative lower absorption were marked by *green circle*. The statistical significance of differences between the four groups was marked. \* $p < 0.05$ , \*\* $p < 0.01$  for Student's *t* test compared to other groups; #Sig < 0.05 for Fisher ratios, compared with between-group and within-group

255.0848, 187.1449, 191.0409, 175.0485, 378.9265, 563.1384, 617.4423, and 601.3859 at MS<sup>2</sup> which were

approximately 16 Da (– O), 32 Da (– 2O) or 48 Da (– 3O) lower than corresponding ions of eriodictyol, diosmetin,

hesperetin, luteolin, apigenin, xanthotoxol, scoparone, sinensetin, kaempferitrin, and rutin. Therefore, they were identified tentatively as hydroxylates and dehydroxylates of prototypical compounds and isomers.

#### *Methoxylated and demethoxylated metabolites*

As shown in Table 2, M29, M33, M34, and M38 exhibited the  $[M + H]^+$  ions at  $m/z$  317.0453, 300.8961, 300.8854, and 233.0639 with formula  $C_{16}H_{12}O_7$ ,  $C_{16}H_{12}O_6$ , and  $C_{12}H_8O_5$  and were eluted at 9.863, 8.537, 8.626, and 9.161 min, respectively, which was approximately 30 Da more than luteolin, apigenin, and xanthotoxol; they were speculated as products of methoxylated metabolites (+  $OCH_2$ ) compared with these prototypical compounds. Metabolites M06, M55, M58, and M60, with  $[M + H]^+$  ions at  $m/z$  271.1385, 359.1934, 364.9185, and 334.838, were eluted at 8.725, 8.993, 10.798, and 8.782 min, respectively. They were 30 Da or 60 Da less than diosmetin, 5-demethylnobiletin, and sinensetin with formula  $C_{15}H_{10}O_5$ ,  $C_{19}H_{18}O_7$ , and  $C_{19}H_{18}O_6$ , suggesting the loss of one or two methoxyl moiety.

#### *Methylated and demethylated metabolites*

Metabolites M13, M46, M47, and M57 were detected at 8.908, 8.76, 8.647, and 8.845 min. They generated the protonated molecule ion at  $m/z$  289.1879 ( $C_{15}H_{12}O_6$ ), 396.7909 ( $C_{19}H_{18}O_8$ ), 368.8728 ( $C_{17}H_{14}O_8$ ), and 380.7709 ( $C_{19}H_{18}O_7$ ), which were 14 Da ( $-CH_2$ ), 28 Da ( $-C_2H_4$ ), or 56 Da ( $-C_4H_8$ ) less than that of hesperetin, nobiletin, and sinensetin, suggesting that they were demethylated products of these prototypical compounds. Metabolites M09-M11, M14-M16, M21, M22, M24-M26, M37, M48-M50, and M65 were speculated to be  $C_{17}H_{14}O_6$ ,  $C_{18}H_{16}O_6$ ,  $C_{18}H_{18}O_6$ ,  $C_{17}H_{16}O_5$ ,  $C_{16}H_{12}O_6$ ,  $C_{17}H_{14}O_6$ ,  $C_{12}H_8O_4$ ,  $C_{22}H_{24}O_8$ ,  $C_{23}H_{26}O_8$ , and  $C_{29}H_{34}O_{16}$  according to their HRMS spectral data. They were 14 Da (+  $CH_2$ ) or 28 Da (+  $C_2H_4$ ) higher than that of diosmetin, hesperetin, naringenin, luteolin, xanthotoxol, nobiletin, and rutin and were deduced as methoxylated metabolites.

#### *Conjugated metabolites*

With their conjugation on the hydroxy group of the benzene ring, we identified sulfate conjugates that were approximately 80 or 96 Da higher than prototypical compounds, such as M04 (eriodictyol +  $SO_3$ ), M12 (diosmetin +  $SO_3$ ), M23 (naringenin + O +  $SO_3$ ), M30 (luteolin +  $SO_3$ ), M40 (xanthotoxol + O +  $SO_3$ ), M43 (scoparone +  $SO_3$ ) and M53 (nobiletin + O +  $SO_3$ ); glucuronide conjugates, such as M22 (naringenin + Glu), M39 (xanthotoxol + O + Glu), M44 (scoparone + O + Glu), M51, and M52 (nobiletin + Glu), were detected as 176 or 192 Da more than that of prototypical compounds; and the

sulfate and glucuronide conjugates, such as M19 (hesperetin +  $SO_3$  + Glu) and M54 (nobiletin +  $SO_3$  + Glu), were approximately 256 Da more than that of prototypical compounds.

## Discussion

TCM is a complex system that exerts its therapeutic effect through the synergistic activity of multiple characteristic constituents. For the constituents absorbed into the blood, which have the opportunity to show bioactivities, a novel strategy based on pseudotargeted metabolomics for screening of QC-markers was developed. The pseudotargeted method which integrates the advantages of both targeted and untargeted methods is demonstrated to be a comprehensive strategy with high-quality and information-abundant data. Researchers, however, often ignore the importance of the prototype constituents with lower absorption, which might act on a converted type. Therefore, it is vital to pay much attention to the design of the pseudotargeted metabolomics strategy developed for screening QC-markers, as any prototype or converted metabolite in the blood will greatly reflect the overall efficiency of TCMs. Due to the structure diversities of the characteristic constituents in TCMs, the bioactivity and absorption of the prototypic constituents exhibit obvious structure-dependence. These may be attributed to drug interaction with intestinal microbiota, CYP-mediated drug metabolism, and their intrinsic chemical properties. To our knowledge, the host biotransformation systems include phase I and phase II reactions. The phase I metabolism, including methoxylation, methylation, hydroxylation, and hydrolysis, is mainly mediated by CYP enzymes in the liver, gut, and other tissues. The phase II metabolism is the conjugation reaction, including glucuronidation and sulfonation.<sup>14</sup> Accordingly, a total of 66 metabolites were convincingly identified, including 52 phase I metabolites and 14 phase II metabolites in rat plasma. The global absorption and in vivo biotransformation process after orally administrated with standard extracts of *Citrus* TCMs was depicted in a systematic manner, as shown in Fig. 3.

The gastrointestinal microbiota can be considered as a site with huge biotransformational capacity of drugs, including hydrolysis and glycosylation. Hydrolysis should directly lead to a decrease in the absorption of glycosides [14]. Because of the hydrolysis of the gastrointestinal microbiota, glycosides as rutin and kaempferitrin exhibited lower absorption, while contributing to the content of their aglycone with the quercetin and kaempferol detected in the blood in “Metabolite identification and biotransformation” section. In addition, polyphenols, such as luteolin, scoparone, and eriodictyol which show relatively high absorption in this study, may affect the binding of microorganisms and other microorganisms by capturing metal ions (such as iron and cobalt) of metalloenzymes in intestinal microbial cells, resulting in the property of chelating

**Table 2** Mass spectral data and biotransformation of prototypical compounds screening and identification

| ID  | RT (min) | Meas. $m/z$<br>([M + H] <sup>+</sup> ) | Meas. $m/z$<br>([M + Na] <sup>+</sup> ) | Mass error<br>(ppm) | Mass shift<br>(Da) | Formula   | EF                                | IPS (%) | CFIs          | Prototype (P)                      |
|-----|----------|--|---|---------------------|--------------------|---|-----------------------------------|---------|---------------|------------------------------------|
| M1  | 8.873    | 305.2081                               | 327.2081                                | 2.519               | 16.0049            | C <sub>15</sub> H <sub>12</sub> O <sub>7</sub>    | P + O                             | 96.0    | 289, 275, 246 | Eriodictyol                        |
| M2  | 9.715    | 257.0834                               | 279.0834                                | 3.484               | -32.1198           | C <sub>15</sub> H <sub>12</sub> O <sub>4</sub>    | P-2O                              | 98.3    | 239, 190      | Eriodictyol                        |
| M3  | 8.898    | 321.2031                               | 343.2031                                | 1.161               | 31.9999            | C <sub>15</sub> H <sub>12</sub> O <sub>8</sub>    | P + 2O                            | 95.2    | 305, 279, 247 | Eriodictyol                        |
| M4  | 7.643    | 369.0745                               | 391.0745                                | 3.001               | 79.8713            | C <sub>15</sub> H <sub>12</sub> O <sub>9</sub> S  | P + SO <sub>3</sub>               | 99.3    | 350, 214      | Eriodictyol                        |
| M5  | 8.725    | 271.1385                               | 293.1385                                | 3.001               | -30.0746           | C <sub>15</sub> H <sub>10</sub> O <sub>5</sub>    | P-O-CH <sub>2</sub>               | 99.3    | 267, 249, 165 | Diosmetin                          |
| M6  | 8.651    | 317.0239                               | 339.0239                                | 3.491               | 15.8108            | C <sub>16</sub> H <sub>12</sub> O <sub>7</sub>    | P + O                             | 98.7    | 285, 217      | Diosmetin                          |
| M7  | 10.588   | 269.1756                               | 291.1756                                | 3.491               | -32.0375           | C <sub>16</sub> H <sub>12</sub> O <sub>4</sub>    | P-2O                              | 98.7    | 263, 194      | Diosmetin                          |
| M8  | 11.925   | 253.1807                               | 275.1807                                | 3.446               | -48.0324           | C <sub>16</sub> H <sub>12</sub> O <sub>3</sub>    | P-3O                              | 98.9    | 217, 179, 131 | Diosmetin                          |
| M9  | 9.652    | 315.0868                               | 337.0868                                | 3.446               | 13.8737            | C <sub>17</sub> H <sub>14</sub> O <sub>6</sub>    | P + CH <sub>2</sub>               | 98.9    | 291, 229      | Diosmetin                          |
| M10 | 12.192   | 315.0875                               | 337.0875                                | 3.446               | 13.8744            | C <sub>17</sub> H <sub>14</sub> O <sub>6</sub>    | P + CH <sub>2</sub>               | 98.9    | 259, 241, 205 | Diosmetin                          |
| M11 | 13.93    | 329.1032                               | 351.1032                                | 3.446               | 27.8901            | C <sub>18</sub> H <sub>16</sub> O <sub>6</sub>    | P + C <sub>2</sub> H <sub>4</sub> | 98.9    | 211, 115      | Diosmetin                          |
| M12 | 7.1902   | 381.0244                               | 403.0244                                | 3.235               | 79.8113            | C <sub>16</sub> H <sub>12</sub> O <sub>9</sub> S  | P + SO <sub>3</sub>               | 98.3    | 313, 245, 207 | Diosmetin                          |
| M13 | 8.908    | 289.1879                               | 311.1879                                | 3.235               | -14.0045           | C <sub>15</sub> H <sub>12</sub> O <sub>6</sub>    | P-CH <sub>2</sub>                 | 98.3    | 263, 246, 229 | Hesperetin                         |
| M14 | 9.384    | 331.1122                               | 353.1122                                | 3.236               | 27.9198            | C <sub>18</sub> H <sub>18</sub> O <sub>6</sub>    | P + C <sub>2</sub> H <sub>4</sub> | 98.0    | 213, 153      | Hesperetin                         |
| M15 | 9.616    | 331.0609                               | 353.0609                                | -1.378              | 27.8685            | C <sub>18</sub> H <sub>18</sub> O <sub>6</sub>    | P + C <sub>2</sub> H <sub>4</sub> | 98.4    | 261, 224      | Hesperetin                         |
| M16 | 9.758    | 331.1559                               | 353.1559                                | 2.817               | 27.9635            | C <sub>18</sub> H <sub>18</sub> O <sub>6</sub>    | P + C <sub>2</sub> H <sub>4</sub> | 97.6    | 324, 280, 226 | Hesperetin                         |
| M17 | 11.613   | 261.1132                               | 283.1132                                | 3.232               | -42.0792           | C <sub>16</sub> H <sub>14</sub> O <sub>4</sub>    | P-2O                              | 99.2    | 249, 196      | Hesperetin                         |
| M18 | 12.362   | 261.1131                               | 283.1131                                | 3.232               | -42.0793           | C <sub>16</sub> H <sub>14</sub> O <sub>4</sub>    | P-2O                              | 99.2    | 241, 205      | Hesperetin                         |
| M19 | 7.655    | 559.022                                | 581.022                                 | 2.806               | 255.8296           | C <sub>22</sub> H <sub>22</sub> O <sub>15</sub> S | P + SO <sub>3</sub> + Glu         | 98.6    | 517, 350, 214 | Hesperetin                         |
| M20 | 9.697    | 301.0711                               | 323.0711                                | 2.806               | 27.9493            | C <sub>17</sub> H <sub>16</sub> O <sub>5</sub>    | P + C <sub>2</sub> H <sub>4</sub> | 98.6    | 242, 219      | Naringenin                         |
| M21 | 15.49    | 301.0719                               | 323.0719                                | 2.806               | 27.9501            | C <sub>17</sub> H <sub>16</sub> O <sub>5</sub>    | P + C <sub>2</sub> H <sub>4</sub> | 98.6    | 241, 220      | Naringenin                         |
| M22 | 7.479    | 449.012                                | 471.012                                 | 2.806               | 175.8902           | C <sub>15</sub> H <sub>12</sub> O <sub>5</sub>    | P + Glu                           | 98.6    | 423, 381, 273 | Naringenin                         |
| M23 | 7.724    | 369.0745                               | 391.0745                                | 2.806               | 95.9527            | C <sub>15</sub> H <sub>12</sub> O <sub>5</sub>    | P + O + SO <sub>3</sub>           | 98.6    | 350, 214      | Naringenin                         |
| M24 | 11.167   | 316.1403                               | 338.1403                                | -1.821              | 28.2394            | C <sub>17</sub> H <sub>14</sub> O <sub>6</sub>    | P + C <sub>2</sub> H <sub>4</sub> | 95.4    | 196, 142      | Luteolin                           |
| M25 | 9.473    | 302.1221                               | 324.1221                                | -0.502              | 14.2212            | C <sub>16</sub> H <sub>12</sub> O <sub>6</sub>    | P + CH <sub>2</sub>               | 97.6    | 258, 227      | Luteolin                           |
| M26 | 10.409   | 324.1245                               | 346.1245                                | -1.445              | 14.2236            | C <sub>16</sub> H <sub>12</sub> O <sub>6</sub>    | P + CH <sub>2</sub>               | 98.9    | 233, 143      | Luteolin                           |
| M27 | 9.641    | 256.1035                               | 278.1035                                | -1.277              | -31.7974           | C <sub>15</sub> H <sub>10</sub> O <sub>4</sub>    | P-2O                              | 98.8    | 247, 230, 203 | Luteolin                           |
| M28 | 9.83     | 256.1206                               | 278.1206                                | -0.888              | -31.7803           | C <sub>15</sub> H <sub>10</sub> O <sub>4</sub>    | P-2O                              | 97.4    | 246, 187, 228 | Luteolin                           |
| M29 | 9.863    | 317.0453                               | 339.0453                                | -2.210              | 29.1444            | C <sub>15</sub> H <sub>10</sub> O <sub>6</sub>    | P + O + CH <sub>2</sub>           | 98.9    | 287, 273, 218 | Luteolin                           |
| M30 | 5.524    | 368.2551                               | 390.2551                                | 1.471               | 80.3542            | C <sub>15</sub> H <sub>10</sub> O <sub>6</sub>    | P + SO <sub>3</sub>               | 95.6    | 188, 143, 120 | Luteolin                           |
| M31 | 8.667    | 286.9081                               | 308.9081                                | 3.289               | 15.9492            | C <sub>15</sub> H <sub>10</sub> O <sub>6</sub>    | P + O                             | 93.3    | 248, 234, 216 | Apigenin                           |
| M32 | 9.562    | 255.0848                               | 277.0848                                | 1.443               | -15.8741           | C <sub>15</sub> H <sub>10</sub> O <sub>4</sub>    | P-O                               | 96.1    | 213, 153      | Apigenin                           |
| M33 | 8.537    | 300.8961                               | 322.8961                                | 0.052               | 29.9372            | C <sub>16</sub> H <sub>12</sub> O <sub>6</sub>    | P + O + CH <sub>2</sub>           | 97.1    | 271, 226      | Apigenin                           |
| M34 | 8.626    | 300.8854                               | 322.8854                                | 4.002               | 29.9265            | C <sub>16</sub> H <sub>12</sub> O <sub>6</sub>    | P + O + CH <sub>2</sub>           | 97.1    | 271, 246      | Apigenin                           |
| M35 | 9.925    | 187.1449                               | 209.1449                                | 4.002               | -15.9006           | C <sub>11</sub> H <sub>6</sub> O <sub>3</sub>     | P-O                               | 97.1    | 163, 135      | Xanthotoxol                        |
| M36 | 8.752    | 219.0272                               | 241.0272                                | 4.228               | 15.9817            | C <sub>11</sub> H <sub>6</sub> O <sub>5</sub>     | P + O                             | 95.3    | 182, 170, 136 | Xanthotoxol                        |
| M37 | 9.607    | 217.1191                               | 239.1191                                | -1.000              | 14.0736            | C <sub>12</sub> H <sub>8</sub> O <sub>4</sub>     | P + CH <sub>2</sub>               | 95.7    | 209, 130      | Xanthotoxol                        |
| M38 | 9.161    | 233.0639                               | 255.0639                                | 3.382               | 30.0184            | C <sub>12</sub> H <sub>8</sub> O <sub>5</sub>     | P + O + CH <sub>2</sub>           | 95.3    | 198, 169      | Xanthotoxol                        |
| M39 | 6.765    | 395.0402                               | 417.0402                                | 2.919               | 191.9947           | C <sub>17</sub> H <sub>14</sub> O <sub>10</sub>   | P + O + Glu                       | 89.5    | 327, 271, 219 | Xanthotoxol                        |
| M40 | 5.742    | 299.1274                               | 321.1274                                | 1.518               | 96.0819            | C <sub>11</sub> H <sub>6</sub> O <sub>8</sub> S   | P + O + SO <sub>3</sub>           | 96.0    | 274, 171      | Xanthotoxol                        |
| M41 | 8.864    | 191.0409                               | 213.0409                                | 3.600               | -16.0781           | C <sub>11</sub> H <sub>10</sub> O <sub>3</sub>    | P-O                               | 97.5    | 173, 150      | Scoparone                          |
| M42 | 8.963    | 175.0485                               | 197.0485                                | 3.291               | -32.0705           | C <sub>11</sub> H <sub>10</sub> O <sub>2</sub>    | P-2O                              | 93.5    | 163, 153      | Scoparone                          |
| M43 | 7.591    | 287.0711                               | 309.0711                                | 3.291               | 79.9521            | C <sub>11</sub> H <sub>10</sub> O <sub>7</sub> S  | P + SO <sub>3</sub>               | 93.5    | 245, 207, 189 | Scoparone                          |
| M44 | 6.161    | 399.1182                               | 421.1182                                | 3.291               | 191.9992           | C <sub>17</sub> H <sub>18</sub> O <sub>11</sub>   | P + O + Glu                       | 93.5    | 341, 273, 223 | Scoparone                          |
| M45 | 8.805    | 440.7268                               | 462.7268                                | 2.389               | 15.8538            | C <sub>21</sub> H <sub>22</sub> O <sub>9</sub>    | P + O(+O + CH <sub>2</sub> )      | 96.3    | 398, 382, 340 | Nobiletin<br>(5-demethylnobiletin) |

**Table 2** (continued)

| ID  | RT (min) | Meas. $m/z$<br>( $[M + H]^+$ ) | Meas. $m/z$<br>( $[M + Na]^+$ ) | Mass error<br>(ppm) | Mass shift<br>(Da) | Formula               | EF                    | IPS (%) | CFIs          | Prototype (P)                      |
|-----|----------|--------------------------------|---------------------------------|---------------------|--------------------|-----------------------|-----------------------|---------|---------------|------------------------------------|
| M46 | 8.76     | 374.7909                       | 396.7909                        | 2.389               | -28.0821           | $C_{19}H_{18}O_8$     | $P-C_2H_4(-CH_2)$     | 96.3    | 351, 337      | Nobiletin<br>(5-demethylnobiletin) |
| M47 | 8.647    | 346.8728                       | 368.8728                        | 4.223               | -56.0002           | $C_{17}H_{14}O_8$     | $P-C_4H_8(-C_3H_6)$   | 97.1    | 353, 301      | Nobiletin<br>(5-demethylnobiletin) |
| M48 | 9.669    | 417.0993                       | 439.0993                        | 4.223               | 14.2263            | $C_{22}H_{24}O_8$     | $P + CH_2(+C_2H_4)$   | 97.1    | 373, 338, 252 | Nobiletin<br>(5-demethylnobiletin) |
| M49 | 8.938    | 438.8826                       | 460.8826                        | 3.014               | 14.0096            | $C_{22}H_{24}O_8$     | $P + CH_2(+C_2H_4)$   | 93.8    | 423, 365      | Nobiletin<br>(5-demethylnobiletin) |
| M50 | 9.785    | 409.0986                       | 431.0986                        | 3.343               | 28.2256            | $C_{23}H_{26}O_8$     | $P + C_2H_4(+C_3H_6)$ | 93.5    | 393, 335      | Nobiletin<br>(5-demethylnobiletin) |
| M51 | 8.403    | 600.8843                       | 622.8843                        | 4.119               | 176.0113           | $C_{27}H_{30}O_{14}$  | $P + Glu$             | 96.3    | 531, 431      | Nobiletin                          |
| M52 | 7.768    | 578.8596                       | 600.8596                        | 4.119               | 175.9866           | $C_{27}H_{30}O_{14}$  | $P + Glu$             | 96.3    | 588, 419, 336 | Nobiletin                          |
| M53 | 4.711    | 498.8147                       | 520.8147                        | 3.944               | 95.9417            | $C_{21}H_{22}O_{12}S$ | $P + O + SO_3$        | 98.3    | 419, 137      | Nobiletin                          |
| M54 | 7.744    | 658.8708                       | 680.8708                        | 4.252               | 255.9978           | $C_{27}H_{30}O_{17}S$ | $P + SO_3 + Glu$      | 93.0    | 583, 369      | Nobiletin                          |
| M55 | 8.993    | 359.1934                       | 381.1934                        | 3.550               | -29.9641           | $C_{19}H_{18}O_7$     | $P-O-CH_2$            | 97.7    | 337, 307, 273 | 5-Demethylnobiletin                |
| M56 | 8.674    | 404.8314                       | 426.8314                        | 3.343               | 15.9739            | $C_{20}H_{20}O_9$     | $P + O$               | 92.1    | 413, 327, 287 | 5-Demethylnobiletin                |
| M57 | 8.845    | 358.7709                       | 380.7709                        | 3.343               | -14.1046           | $C_{19}H_{18}O_7$     | $P-CH_2$              | 92.1    | 341, 323, 207 | Sinensetin                         |
| M58 | 10.798   | 342.9185                       | 364.9185                        | 3.456               | -29.957            | $C_{19}H_{18}O_6$     | $P-O-CH_2$            | 97.4    | 349, 263      | Sinensetin                         |
| M59 | 8.973    | 356.9265                       | 378.9265                        | 3.351               | -15.949            | $C_{20}H_{20}O_6$     | $P-O$                 | 95.8    | 359, 307, 249 | Sinensetin                         |
| M60 | 8.782    | 312.838                        | 334.838                         | 3.500               | -60.0375           | $C_{18}H_{16}O_5$     | $P-2(O-CH_2)$         | 93.9    | 319, 293      | Sinensetin                         |
| M61 | 10.354   | 563.1384                       | 585.1384                        | 3.500               | -16.2856           | $C_{27}H_{30}O_{12}$  | $P-O$                 | 93.9    | 427, 309, 227 | Sinensetin                         |
| M62 | 9.072    | 309.1794                       | 331.1794                        | 3.840               | -270.2446          | $C_{15}H_{10}O_6$     | $P-2Rha$              | 95.9    | 297, 283      | Kaempferitrin                      |
| M63 | 7.779    | 617.4423                       | 639.4423                        | 3.840               | -15.8785           | $C_{27}H_{30}O_{15}$  | $P-O$                 | 95.9    | 609, 336      | Rutin                              |
| M64 | 7.781    | 579.3859                       | 601.3859                        | 3.840               | -31.9349           | $C_{27}H_{30}O_{14}$  | $P-2O$                | 95.9    | 524, 350      | Rutin                              |
| M65 | 8.026    | 639.816                        | 661.816                         | 3.840               | 28.4952            | $C_{29}H_{34}O_{16}$  | $P + C_2H_4$          | 95.9    | 650, 620      | Rutin                              |
| M66 | 9.117    | 303.1743                       | 325.1743                        | 3.547               | -308.1465          | $C_{15}H_{10}O_7$     | $P-Rutin$             | 92.0    | 299, 277, 257 | Rutin                              |

*meas. m/z* measured mass-to-charge-ratio of protonated, *EF* equivalent formula, *IPS* isotopic pattern score, *CFIs* characteristic fragment ions, *Glu* glucuronic acid

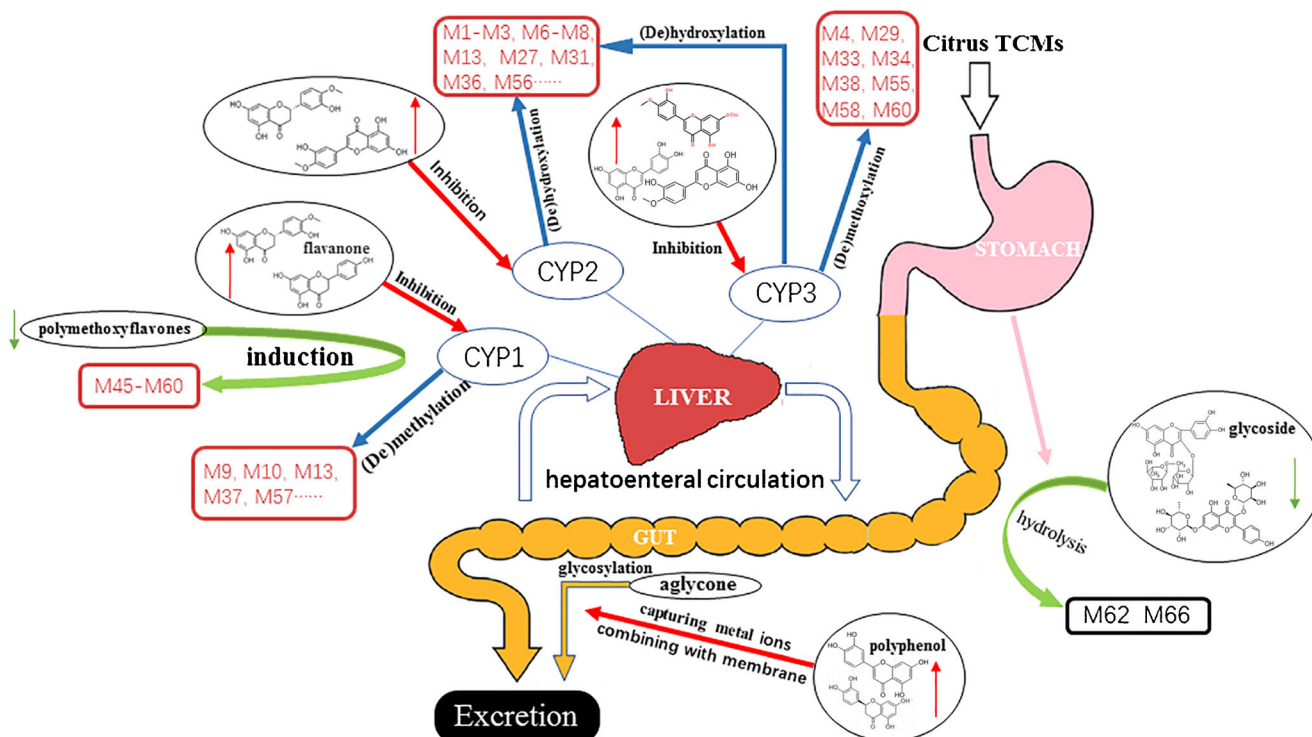


**Fig. 3** Prototypical compounds and metabolites inside the boxes represent the metabolism of in rats' stomach, liver, and gut. The compounds connected by the *red arrow* may cause the relative higher absorption, the *green arrow* may cause the relative lower absorption

with metal ions to form insoluble complexes to inhibit glycosylation in the intestines [15]. For glycosylation in the intestines, the toxicity or activity of the drug is reduced, and the polarity is increased to accelerate the excretion directly, with the flavonoid aglycones, such as acacetin and isosakuranetin, showing relatively weaker absorption in the results of our study. The prototype compounds, including eriodictyol, diosmetin, scoparone, xanthotoxol, hesperetin, naringenin, luteolin, and nobiletin, are conjugated with endogenous molecules (glucuronosyl and sulfo) by host enzyme transfer systems to increase their excretion. In our study, when administered orally, flavonoid glycosides demonstrate lower absorption and total plasma levels compared to aglycones. Thus, the interaction between the gut microbiota and orally administered drugs may modify the structure and function of chemicals and be important in drug investigation.

CYP in the liver and other tissues are a major source of variability in drug pharmacokinetics and response. Functional CYPs belonging to the CYP1, 2, and 3 families are responsible for the biotransformation of most foreign substances, including a large scale of structure diversities in clinical use. The CYP enzymes have indispensable functions in drug metabolism; also, flavonoids are known to have effects on CYP enzymatic activity. Expression of CYP1A2 in the CYP1 family was relatively high in the liver, the main drug metabolic organ, which plays a significant role in the metabolism of several clinically important drugs by catalyzing biotransformations of deethylation and demethylation [16]. Flavanones, including

hesperetin and naringenin, have enhanced absorption, which might be attributed to the inhibition of CYP1A2 [17]. CYP2C9 is the highest expressed member being expressed in the CYP2 family, while CYP2C8 and CYP2C19 are expressed at ~2-fold and 10-fold lower levels, catalyze biotransformations, including deethylation, oxidation, and hydroxylation [16]. Diosmetin inhibits CYP2C8 and CYP2C9 at concentrations similar to those observed after in vivo administration (in the low micromolar range) and may be of potential clinical relevance, since it may cause the higher absorption in this study with drugs metabolized by this CYP [18, 19]. CYP3A4 is in the majority of individuals, is abundantly expressed in the liver, and plays a major role in the metabolism of ~30% of clinically used drugs. The active site of CYP3A4 is large and flexible and can accommodate and metabolize many preferentially lipophilic compounds with the typical pathway of hydroxylation, demethylation, and demethoxylation [16]. In this instance, the polyhydroxylated flavones luteolin and naringenin may inhibit the metabolism of the drug which is catalyzed by CYP3A4, causing the stronger relative absorption [20, 21]. However, polymethoxyflavones, including nobiletin, tangeretin, 5-demethylnobiletin, and sinensetin, exhibited relatively lower absorption in our study, which is consistent with a previous report that this kind of constituent showed low oral bioavailability. The induction of CYP1A1, CYP1A2, and CYP2B enzymatic activity by the polymethoxyflavones might enhance the metabolism of parent constituents. In addition,



hydroxylated polymethoxyflavones have been shown to have a broad spectrum of biological activities, such as anti-inflammatory, anti-cancer, and anti-atherogenic properties, indicated polymethoxyflavones may act on a metabolic type in vivo [22, 23]. This finding indicated that any ignored blood metabolites converted by in vivo biotransformation will greatly influence the overall effect of the specific TCM, which will be based on incomplete and skewed information.

In the present study, targeted metabolomics employing RRLC-QqQ-MS operated in the MRM mode is applied for determination and quantification of 32 prototype metabolites absorbed in the blood. Untargeted metabolomics employing UHPLC-QE Orbitrap HRMS can invariably determine the downstream metabolites' effects on lower blood concentrations of the parent drug in the complex TCMs. Integrating these two methods, pseudotargeted metabolomics methodology was proposed to provide a global insight into the complex process of TCMs in the blood and to characterize the rational screening of potential QC-markers of TCMs.

**Acknowledgements** This study was financially supported by the National Science Foundation of China (Project No. 81573569 and No. 81470177). And also supported by the long-term subsidy mechanism from the Ministry of Finance and the Ministry of Education of PRC for BUCT.

**Compliance with ethical standards** Experiments, which were conducted in a specific pathogen-free (SPF) grade laboratory, were carried out in accordance with the Guide for the Care and Use of Laboratory Animals as adopted and promulgated by the National Health Ministry of China. Protocols for animal experiments had been approved by the Animal Center of the Institute of Basic Theory, China Academy of Chinese Medical Sciences.

**Conflict of interest** The authors confirm that there were no conflicts of interest in performing this study.

## References

1. Wang S. A pre-classification strategy based on UPLC-triple-TOF/MS for metabolic screening and identification of *Radix glehniae* in rats. *Anal Bioanal Chem.* 2016;408:1–14.
2. Barrek S, Paise O, Grenier-Loustalot MF. Analysis of pesticide residues in essential oils of citrus fruit by GC-MS and HPLC-MS after solid-phase extraction. *Anal Bioanal Chem.* 2003;376:157–61.
3. Pujos-Guillot E, Hubert J, Martin JF, Lyan B, Quintana M, Claude S, et al. Mass spectrometry-based metabolomics for the discovery of biomarkers of fruit and vegetable intake: citrus fruit as a case study. *J Proteome res.* 2013;12:1645–59.
4. Dong F, Deng D, Chen H, Cheng W, Li Q, Luo R, et al. Serum metabolomics study of polycystic ovary syndrome based on UPLC-QTOF-MS coupled with a pattern recognition approach. *Anal Bioanal Chem.* 2015;407:4683–95.
5. Chen J, Hou W, Han B, Liu G, Jin G, Li Y, et al. Target-based metabolomics for the quantitative measurement of 37 pathway metabolites in rat brain and serum using hydrophilic interaction ultra-high-performance liquid chromatography–tandem mass spectrometry. *Anal Bioanal Chem.* 2016;408:1–16.
6. Shao Y, Zhu B, Zheng R, Zhao X, Yin P, Lu X, et al. Development of urinary pseudotargeted LC-MS-based metabolomics method and its application in hepatocellular carcinoma biomarker discovery. *J Proteome res.* 2015;14:906–16.
7. Naesens M, Sarwal MM. Molecular diagnostics in transplantation. *Nat Rev Nephrol.* 2010;6:614–28.
8. Zeng H, Liu Z, Zhao S, Shu Y, Song Z, Wang C, et al. Preparation and quantification of the total phenolic products in citrus fruit using solid-phase extraction coupled with high-performance liquid chromatography with diode array and UV detection. *J Sep Sci.* 2016;39:3806–17.
9. Yu J, Wang L, Walzem RL, Miller EG, Pike LM, Patil BS. Antioxidant activity of citrus limonoids, flavonoids, and coumarins. *J Agric Food Chem.* 2005;53:2009–14.
10. Lu Y, Zhang C, Bucheli P, Wei D. Citrus flavonoids in fruit and traditional Chinese medicinal food ingredients in China. *Plant Foods hum Nutr.* 2006;61:57–65.
11. Nogata Y, Sakamoto K, Shiratsuchi H, Ishii T, Yano M, Ohta H. Flavonoid composition of fruit tissues of citrus species. *Biosci Biotechnol Biochem.* 2006;70:178–92.
12. Prasad B, Garg A, Takwani H, Singh S. Metabolite identification by liquid chromatography-mass spectrometry. *TrAC Trends Anal Chem.* 2011;30:360–87.
13. Brink A, Fontaine F, Marschmann M, Steinhuber B, Cece EN, Zamora I, et al. Post-acquisition analysis of untargeted accurate mass quadrupole time-of-flight MSE data for multiple collision-induced neutral losses and fragment ions of glutathione conjugates. *Rapid Commun Mass Sp.* 2014;28:2695–703.
14. Li H, He J, Jia W. The influence of gut microbiota on drug metabolism and toxicity. *Expert Opin Drug Metab Toxicol.* 2016;12:31–40.
15. McDonald M, Mila I, Scalbert A. Precipitation of metal ions by plant polyphenols: optimal conditions and origin of precipitation. *J Agric Food Chem.* 1996;44:599–606.
16. Zanger UM, Schwab M. Cytochrome P450 enzymes in drug metabolism: regulation of gene expression, enzyme activities, and impact of genetic variation. *Pharmacol Ther.* 2013;138:103–41.
17. Pingili R, Vemulapalli S, Mullapudi SS, Nuthakki S, Pendyala S, Kilaru N. Pharmacokinetic interaction study between flavanones (hesperetin, naringenin) and rasagiline mesylate in wistar rats. *Drug Dev Ind Pharm.* 2016;42:1110–7.
18. Quintieri L, Bortolozzo S, Stragliotto S, Moro S, Pavanetto M, Nassi A, et al. Flavonoids diosmetin and hesperetin are potent inhibitors of cytochrome P450 2C9-mediated drug metabolism in vitro. *Drug Metab Pharmacokinet.* 2010;25:466–76.
19. Quintieri L, Palatini P, Moro S, Floreani M. Inhibition of cytochrome P450 2C8-mediated drug metabolism by the flavonoid diosmetin. *Drug Metab Pharmacokinet.* 2011;26:559–68.
20. Quintieri L, Palatini P, Nassi A, Ruzza P, Floreani M. Flavonoids diosmetin and luteolin inhibit midazolam metabolism by human liver microsomes and recombinant CYP 3A4 and CYP3A5 enzymes. *Biochem Pharmacol.* 2008;75:1426–37.
21. Burkina V, Zlabek V, Halsne R, Ropstad E, Zamaratskaia G. In vitro effects of the citrus flavonoids diosmin, naringenin and naringin on the hepatic drug-metabolizing CYP3A enzyme in human, pig, mouse and fish. *Biochem Pharmacol.* 2016;110-111:109–16.
22. Mekjaruskul C, Jay M, Sripanidkulchai B. Modulatory effects of *Kaempferia parviflora* extract on mouse hepatic cytochrome P450 enzymes. *J Ethnopharmacol.* 2012;141:831–9.
23. Mekjaruskul C, Jay M, Sripanidkulchai B. Pharmacokinetics, bio-availability, tissue distribution, excretion, and metabolite identification of methoxyflavones in *Kaempferia parviflora* extract in rats. *Drug Metab Dispos.* 2012;40:2342–53.